Low-cost CATV transmission in fiber-to-the-home networks

van de Water, M.

Award date:
2005

TU/e technische universiteit eindhoven

Low-cost CATV Transmission in Fiber-to-the-Home Networks

Master of Science Thesis

By: Matthijs van de Water

/faculteit elektrotechniek

Eindhoven University of Technology
Faculty of Electrical Engineering
Division of Telecommunication Technology and Electromagnetics
Electro-Optical Communications Group

Low-cost CATV Transmission in Fiber-to-the-Home Networks

Matthijs van de Water

Master of Science Thesis
work carried out from September 2004 to June 2005
at Genexis B.V. Eindhoven

Supervisor:
Ir. J.J.J. Crijns (Genexis B.V.)

Graduation professor:
Prof. Ir. A.M.J. Koonen

The Examinations Committee of the Faculty of Electrical Engineering has authorized the embargo of Appendix F for one year after the publication date of this report.

Abstract

Genexis B.V. is a player in the fiber-to-the-home (FTTH) market. They design equipment for both customer premises and central office, for triple-play (internet, telephony and television) FTTH networks. In this thesis, low-cost and scalable methods of transmitting analog CATV over a point-to-point FTTH network from the central office were examined.

A literature study of the theoretical background has been made regarding the main system performance measures: the carrier-to-noise ratio (CNR), composite second order (CSO) intermodulation distortion and composite triple beat (CTB) intermodulation distortion. We have defined a model that shows the dependence of CNR, CSO and CTB on important system parameters like received optical power and optical modulation index. In order to verify the validity of our model, we measured CNR, CSO and CTB dependence on the system parameters using two directly modulated 1310-nm laser modules. Both two-tone and multi-tone measurements were conducted. The two-tone measurements proved to be not representative for CSO and CTB behavior of an actual system. The multi-tone measurements gave fairly accurate results. Therefore we conclude that in order to measure CSO and CTB performance of the system, we need to perform multi-tone measurements.

Building on this information, four technological solutions for the central office were considered, being 1310 vs. 1550 nm transmission wavelength and direct vs. external modulation of the optical source. These solutions were judged based on the condition that they should be both low-cost and scalable in order to succeed in the highly competitive FTTH market. The two most promising architectures – directly modulated 1310 and 1550 nm – were subjected to link budget calculations and an economical analysis, showing promising implementations of a low-cost, scalable central office solution. In the 1550-nm case, the economical aspects of the use of Erbium-doped fiber amplifiers (EDFAs) was examined to enlarge the link budget and thus the split factor. We conclude that both solutions fit our initial design challenge.

Taking it one step further, the feasibility of building a device for both central office and customer premises that enables the use of a single residential optical fiber to transmit both data and analog CATV has been researched. We have shown that using wavelength division multiplexing (WDM) it is possible to transmit both up- and downstream data and downstream analog CATV over a single optical fiber, while avoiding crosstalk between the different signals. We have identified devices for both customer premises equipment and central office that enable this single fiber solution and we have verified the customer premises side by doing measurements and building a system demonstrator. For the central office a recommendation has been made which enables a single fiber solution, but retains scalability.

Finally, a readily adoptable, low-cost and scalable solution for the transmission of CATV in a point-to-point FTTH network is proposed, as well as a direction for future research.

Contents

Chapter 1

Graduation project description

1.1 Background

Genexis is a relatively new player in the emerging fiber-to-the-home (FTTH) market. It was founded in 2002 and is based in Eindhoven, the Netherlands. The Genexis team is presently still relatively small with 6 full-time employees, but all team members have experience in optical technologies and engineering. In September 2004, Genexis shipped the first customer premises equipment to the Nuenen FTTH project, which was the first large-scale FTTH project in the Netherlands. Genexis designs implementations of FTTH based on point-to-point fiber optic links, providing consumers with high-speed internet access, telephony and analog and digital CATV (triple play). In the consumers home, the Genexis FiberXport® product family connects the optical network to the existing in-home networks. Within this modular triple play concept they designed and developed the NTUO, a broadband CATV receiver module, and the OCG, a data communications module. The OCG is capable of delivering managed 100 Mbit/s standard ethernet and voice-over-IP (VoIP) telephony using a different wavelength for up- and downstream. The wavelengths for data communication are most commonly 1310 and 1550 nm, but can also be 1310 and 1490 nm if data and CATV are combined on a single optical fiber (with CATV at 1550 nm). The NTUO receiver supports both conventional analog CATV and digital video broadcasting (DVB), which it transparently offers to the end-user and therefore does not require a set-top box for analog CATV. The NTUO features a high carrier-to-noise ratio, high optical sensitivity and good noise and distortion performance [1]. Using this NTUO, there are several possibilities to design the central office CATV equipment and the fiber-to-the-home network architecture. The highly competitive FTTH market calls for a scalable and cost-effective CATV solution. It is such a solution, given several preconditions, this M.Sc. project has researched.

1.2 Project Approach

The first part of this research comprised of a literature study about carrying CATV over FTTH networks. The existing techniques and network topologies were examined and the key properties of each were listed and compared. From this literature research, the most promising candidates were selected for further analysis.

Taking a set of preconditions and the results of the literature study into account, the most promising candidates were subjected to comparative measurements of estimated field-performance. Here, link budget and transmitter, splitter and receiver specifications were the important variables.

In the last step of the research, one technique was selected and further detailed. The network topology, economic impact and technical implementation was analyzed in detail. Extended measurements on an entire system were conducted. After this, recommendations for a strategy to

carry CATV efficiently over FTTH was made, including transmitter and receiver technology and network topology. Within this strategy, particular attention was given to the option to deploy a 'triplexer', i.e. a device that splits the three signals on the residential fiber into separate CATV, broadband internet and ISDN-quality telephony signals, which the consumer can connect to their existing equipment.

1.3 Preconditions

The Genexis definition of the FTTH concept introduces some important preconditions, which define boundaries for the subfield of FTTH that has been researched.

1.3.1 Quality of Service

First and most important of all, the perceived quality of service of the consumers existing coaxial CATV connection must be matched or surpassed. This calls for high carrier-to-noise ratios and low distortions as we will see in Chapter 3.

1.3.2 Backward compatibility

Because this technology has to compete with the existing coaxial CATV connection, a switch to FTTH should be as easy as possible. Existing television sets and VCRs, as well as existing coaxial distribution network inside the home should not have to be replaced. This calls for an analog solution, directly compatible with the current coaxial connection, as opposed to digital IP television over an ethernet network. For conventional CATV, this would not require a set-top box (STB) and therefore provides a seamless transfer. The Genexis optical analog CATV receiver provides this functionality and is used in the system measurements of Chapter 4.

1.3.3 Scalability

Furthermore, since FTTH will be introduced gradually, the network topology and central office equipment has to be scalable. It should be possible to connect consumers in batches of as low as 32 connections. Also, this calls for low-cost implementations, because market-prices have to be competitive to existing (coaxial/twisted pair) networks. This will be analyzed in detail in Chapter 5.

1.3.4 Network topology

Because the Genexis FTTH products are based on a point-to-point network topology, the CATV connection has to use this point-to-point network. Since CATV is a broadcast service, we have to find an efficient way to emulate a broadcast or point-to-multipoint network topology on a point-to-point optical network. Current FTTH deployments in the Netherlands use two fibers, one for data and one for CATV. In Chapter 6, we will also look at putting all three services (telephony, internet data and CATV) on a single fiber.

Chapter 2

Introduction into CATV and FTTH networks and techniques

In fiber-to-the-home (FTTH) networks there are several different implementations that can be used to enable consumers to watch television via optical fiber. Some of these implementations are close to the current CATV system, retaining the broadcast network topology and analog signals. Others use dedicated connections from central office to customer premises, either carrying analog signals or digital (IP) streams. In this chapter, we will introduce the most important technological implementations of CATV[1] over fiber.

2.1 Hybrid fiber coax CATV networks

The CATV networks in the Netherlands, most parts of western Europe and some parts of the United States are so-called *hybrid fiber coax* (HFC) networks. This is currently the latest standard of structuring a CATV network and has been rolled out during the last two decades. In HFC, the first part of the distribution network, down to the *central office* (CO), is using optical fiber and optical amplification. The so-called *last mile* from the CO to the customer premises uses coaxial cabling and electrical amplification (see Figure 2.1).

The so-called optical *trunk* features cost-effective amplification, low loss and distortion and enables two-way (data) communication. The signals going over this part of the network can be both analog and digital, or a combination of both. Multiplexing schemes used are *wavelength division multiplexing* (WDM) and *subcarrier multiplexing* (SCM).

In the CO the optical signals are converted back to the electrical domain. If they are digital (MPEG) encoded streams, they will be decoded and prepared for *amplitude modulation* (AM) analog transmission. The analog optical signals will already use AM and can therefore be transparently converted to electrical signals. The different electrical channels, including some locally generated signals (localized information and news channels) are then frequency division multiplexed on a single signal which is compatible with traditional all-electronic CATV signals. The multiplexed signal is then amplified and split and fed to the coaxial part of the distribution network, towards the customer premises.

In this coaxial network that connects the customer premises with the CO, the electrical signal is split and amplified multiple times, end-users are connected with a tree-shaped network. Because the signals are frequency division multiplexed AM *vestigial side band* (VSB) channels, they are compatible with current analog television sets, which can use their tuners to display the desired

[1] We will use the term CATV here in its broadest sense, to indicate a system that transports television signals to the customer premises.

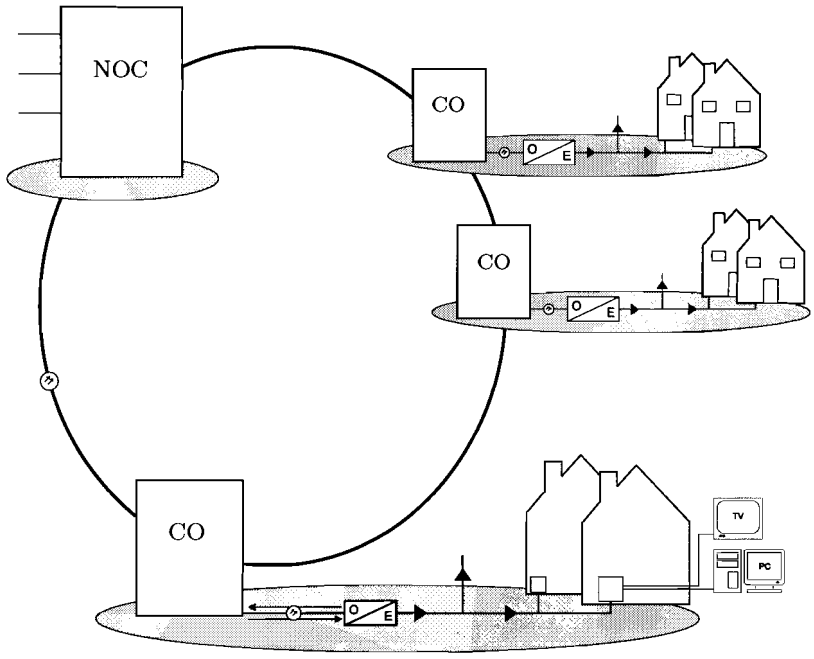

Figure 2.1: A typical HFC network with network operation center (NOC), central offices (CO) and street cabinets (O/E). Internet access uses cable modems.

channel. This HFC network has not only introduced important efficiency improvements for the CATV distributer, in most cases it has also improved end-user picture quality and network capacity (e.g. more channels). Due to the low fiber losses, much lower than those of coaxial cables, many coax intermediate amplifiers can be skipped in the HFC concept, which also yields a sizeable improvement of the CATV signals (less noise, less intermodulation distortions). Another important improvement is that along with this network upgrade, most CATV distributers replaced the RF amplifiers and splitters in the coaxial part of the network with two-way capable devices, enabling two-way data communication. Using *quadrature amplitude modulation* (QAM) these digital signals are modulated and then *subcarrier multiplexed* (SCM) with the AM-VSB signals so that the upstream digital channel is located below the CATV band and the downstream digital channels are above or in empty bands within the CATV band (see Fig. 2.2). This does not only enable internet access using cable modems, but it also clears the way for digital television (see Section 2.3).

2.2 Introducing fiber-to-the-home

With FTTH, we replace the coaxial distribution part of the CATV network by optical fibers. This optical distribution network can either use a point-to-point or point-to-multipoint structure from the CO, as we will see later. The important thing is that with FTTH people have an optical fiber connection to the central office that does not only carry CATV signals, but also telephony and internet data. The provisioning of these three communication services by a single provider is referred to as *triple-play*. Advantages of the optical fiber over the coaxial cable are not only related to available bandwidth, which is several orders of magnitude higher, but also to reduced link-loss and therefore reduced need for amplification in the last part of the network, which implies less noise and less nonlinear distortions.

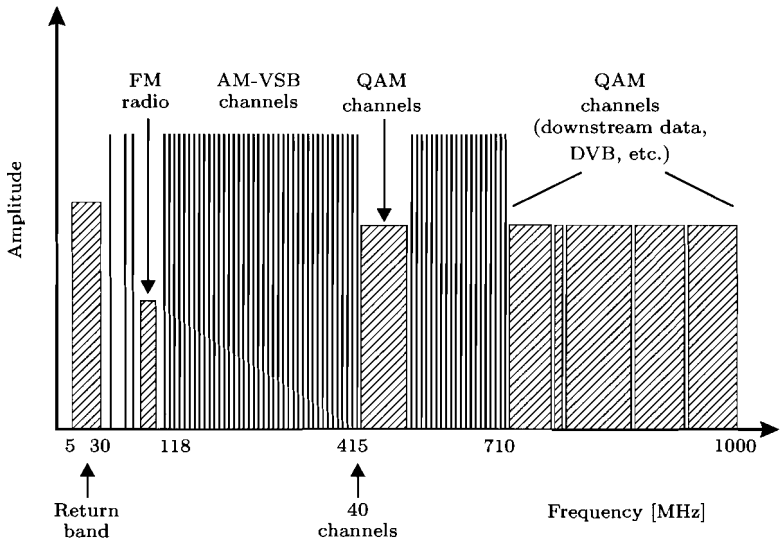

Figure 2.2: CATV spectrum with an example of a typical channel plan, including various digital channels and two-way communication.

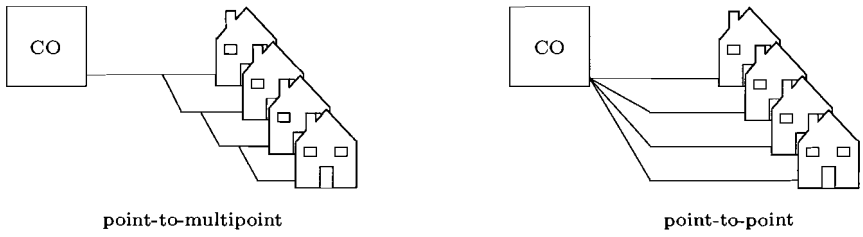

Figure 2.3: Point-to-multipoint (PON) network architecture versus point-to-point network architecture.

2.2.1 Passive Optical Network

Generally speaking, there are two types of optical access network structures for FTTH: the *passive optical network* (PON), which is a point-to-multipoint architecture and the point-to-point architecture (see Fig. 2.3). In a PON a fiber from the CO connects a group of houses, by means of passive optical splitting. This is a tree-shaped network, where the number of houses connected to one branch is limited by the link budget (e.g. the fiber length and number of splitters) and multiple access technique properties. In a PON, the multiple access technique that is most often used is *time division multiple access* (TDMA), which offers a cost-effective connection. *Wavelength division multiple access* (WDMA) could also be used in combination with optical wavelength routing and TDMA to achieve higher bandwidth, but because of the high cost of WDM equipment, WDM is currently only used to separate up- and downstream signals. We can see that therefore the multiple access technique imposes a limit on the number of houses that can be connected to one branch, because they share their bandwidth using TDMA. TDMA also poses problems with data security, all houses connected to a single branch essentially also receive data for all other houses. There are four different PON standards, namely the ATM PON (APON), Ethernet PON (EPON), Broadband PON (BPON) and Gigabit PON (GPON). An APON uses Asynchronous Transfer Mode (ATM) as the bearer protocol and was the first PON standard. Later, the name BPON was introduced, because APON made people believe PON could only support ATM. The

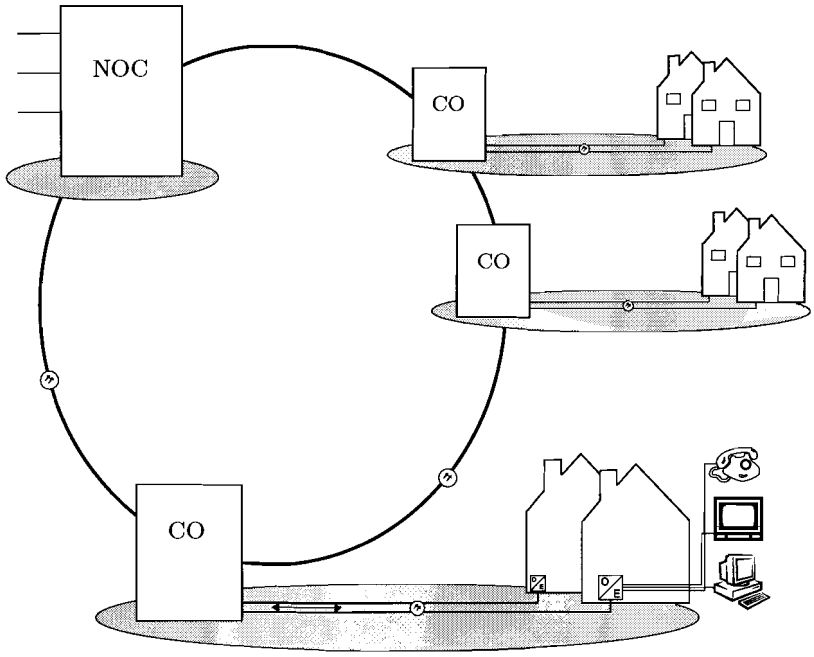

Figure 2.4: A typical FTTH network with network operation center (NOC), central offices (CO) and customer premises equipment (O/E).

latest additions to the PON family of standards are EPON (defining an Ethernet point-to-point access network over a point-to-multipoint passive optical link) and GPON, which defines an open standard (including but not limited to Ethernet) to enable gigabit data communication over PONs.

2.2.2 Point-to-point network

In this thesis we will further study the point-to-point network architecture, as this is the common architecture for FTTH in the Netherlands and the Genexis product line is based on this point-to-point architecture. Figure 2.4 shows an overview of a typical point-to-point FTTH network (cf. Fig. 2.1). The optical trunk is identical to the one in a HFC network, but the tree-shaped coaxial broadcast network with splitters and amplifiers is replaced with point-to-point optical fibers. This means that each house has a dedicated optical connection to the CO. Data security is therefore inherent to this architecture and we have the entire bandwidth of the optical fiber available for current and future services. We will use different wavelengths for downstream CATV, downstream data and upstream data, a technique referred to as coarse WDM.

It is interesting to note that with both HFC and FTTH architectures, although the trunk and the feeder networks are optical, in the CO the signal is still converted to the electrical domain. This is because channels from different sources and with different compositions (analog/digital) have to be multiplexed together, which is most conveniently done in the electrical domain.

Now that we have generally explored the network architectures of FTTH, we will focus on CATV signals in FTTH. In the next two sections we will make an initial distinction between analog and digital signals. As we have learned, from a traditional CATV point of view, the use of analog signals is not only straightforward, but also already widely used in the trunk part of HFC networks. But since more and more services are becoming digital (first telephony with ISDN and later VoIP, now CATV with DVB and HDTV), the exclusive use of digital signals is an option that should

also be considered. We will look at the possibilities of both analog and digital CATV delivery over optical fiber and discuss their advantages.

2.3 Digital TV

Looking at the future, digital television is coming. *Digital Video Broadcasting* (DVB) and *High Definition Television* (HDTV) are two well-defined universally adopted standards that are gaining popularity. Also IPTV services implementing true *Video on Demand* (VoD) and *Pay-Per-View* (PPV) video delivery are becoming more and more interesting as more people get access to a broadband internet connection. Since digital television is the future, it seems obvious that it should be part of access networks of the future.

All forms of digital television make use of some form of encoding to reduce the vast amount of bits needed to digitize a video signal. The most widely used and universally adopted are the MPEG standards of the Moving Picture Experts Group, which is constantly working to reduce bandwidth requirements and enhance picture quality. They have defined several standards for different applications, ranging from DVD- to broadcast-quality video. These MPEG streams still need a lot of bandwidth, which has important implications when designing a broadcast digital CATV system. A broadcast quality CATV channel would require about 115 Mbit/s without compression (8 bit A/D) and still 2.048 Mbit/s using MPEG2 compression. Broadcasting 42 different channels at the same time, while keeping bandwidth available for more advanced services like VoD and HDTV is not trivial, even with the vast amount of bandwidth available in FTTH.

Something else that all digital CATV options have in common is their dependance on set-top boxes (STBs) for each traditional television set and VCR. This STB converts the digital video signal (MPEG) into composite video (CVBS), which the TV can handle. Disadvantages of the use of STBs include having to use the STB remote control to switch channels and needing a different STB for each TV-set and VCR in the house. The functionality of STBs will most likely be integrated into future TV sets, so this is mainly a transitional problem. For the immediate future however, the cost of one or more STBs per household is not something the consumer wants to pay for when switching from analog CATV to digital CATV in FTTH, when no additional services or better quality are offered.

In this section we will look at two different means of delivering digital television over FTTH. We can either use an analog connection and QAM to broadcast DVB or an ethernet connection to multicast IPTV.

2.3.1 Digital video broadcasting

The DVB project defines digital broadcasting standards for satellite (DVB-S), cable (DVB-C) and terrestrial (DVB-T) that are already widely in use. DVB is a logical successor of current AM-VSB analog CATV. It is transmitted over the same analog link, and uses QAM to modulate the digital channels which are multiplexed with the AM-VSB channels using FDM (see also Fig. 2.2). This method is already in use in current HFC CATV networks, delivering both conventional analog CATV and digital television channels simultaneously. For conventional TV sets, a STB is needed to decode the MPEG digital channels. This standard uses the same coaxial cables as conventional analog CATV and its installation is therefore as easy as plugging some cables into a STB. The backward compatibility this digital television standard offers is one of its key features and the reason for its succes with both cable providers and end users. Within the DVB standard, it is also possible to define high-quality HDTV channels and using the upstream band in the CATV spectrum that is normally used for cable modems, even VoD and PPV are possible.

2.3.2 IP television

If we look at the services a triple play FTTH system must deliver, internet and telephony are digital two-way communication services, that use an ethernet network. IPTV uses this same ethernet network to deliver CATV to the customer premises. IPTV uses MPEG compression and the resulting digital stream is packaged in IP packets and transmitted over the ethernet connection just as the telephony VoIP streams are.

As we have seen before, it would require a lot of bandwidth to transmit 42 different channels at the same time. If these 42 channels would have to be available simultaneously, they would eat up almost 100 Mbit/s. Because nobody watches all channels at the same time and this would require a lot more high bandwidth IP switching in the central office (and thus more expensive equipment), a maximum of three or four broadcast channels are usually transported to the users home. This still requires expensive broadband IP switches in the central office, to switch up to four IP multicast streams to each home. IP television can however be totally interactive, which opens the door to endless video-based services.

2.4 Analog TV

2.4.1 Frequency modulation

Because of the enormous installed base of analog TV sets, analog CATV has to be supported for many years. Since most CATV networks currently use optical fibers in their trunk (HFC), which transport the CATV signals in analog form, keeping them that way for FTTH seems logical. The disadvantage of AM modulation, which is primarily used in the trunk network of HFC, is the stringent CNR and distortion requirements. The corresponding high cost per subscriber led to some trials of using FM modulation, which is also used in satellite television. FM relaxes the signal requirements and thus lowers the cost for optical equipment. A satellite receiver or STB for each TV-set is needed, but these are more readily available and cheaper than the specialized digital STBs needed for digital CATV. The big disadvantage of using FM is that it requires far more bandwidth (more than 20 MHz per channel) than AM-VSB, which is why it was never adopted as a replacement for AM-VSB in FTTH.

2.4.2 Amplitude modulation

When new DFB lasers which could meet the linearity and distortion requirements of AM modulation were developed and cost of other optical components (amplifiers, splitters) started to drop, AM-VSB television in FTTH became a feasible option. Currently the CATV signals entering a CO are mostly optical AM-VSB sub-carrier multiplexed signals. These can be directly passed onto the coaxial feeder network, over which AM-VSB has been transmitted since the beginning op CATV networks. If this last copper part of the network is replaced with optical fiber, it seems logical to feed this optical trunk signal directly into the feeder fiber. The electro-optical conversion would be straightforward and the consumer can connect his existing equipment and in-house infrastructure to this unit (Customer Premises Equipment, CPE), without the use of STBs. These advantages in backward compatibility and transparency are the mean reasons why we will analyze analog optical CATV transmission in more detail.

Chapter 3

Theory of analog optical communication

In this chapter we will investigate the theoretical details of analog optical communication using laser diodes. We will discus the details of the analog optical link and the challenges related to the use of frequency division multiplexing to transmit multiple RF channels using a single optical carrier. Detailed expressions of the *carrier-to-noise ratio* (CNR) and harmonic and intermodulation distortions will be derived.

3.1 Overview of the analog link

An analog optical communication link typically consists of a laser transmitter, optical fiber, optical amplifier(s) and photo detector receiver. Each section of this link has its own properties with respect to power conversion and noise contribution.

To transmit an analog signal using a laser diode, a technique called *direct intensity modulation* is often used: the laser driving current is varied around a bias point, resulting in a variation in the intensity of the optical output power. The intensity of the laser light directly reflects the amplitude of the input signal in a linear relationship. Using direct modulation, one can directly send the information of an analog signal in baseband. For CATV purposes, it is however more efficient to first modulate an RF carrier with the signal and then use the result to intensity modulate the laser. The modulation used can be standard amplitude modulation (AM), frequency modulation (FM) or phase modulation (PM). For CATV systems, we will focus on AM modulation, because existing CATV systems already use AM-VSB and this signal can be directly fed to existing television sets (see the discussion in Chapter 2).

In Fig. 3.1 a schematic overview of the communication system is given. Once the electrical signal is transferred into the optical domain and coupled into the optical fiber, it can optionally be amplified (at 1550 nm Erbium doped fiber amplifiers, EDFAs, can be used). After some length of fiber and possibly some optical amplification stages, the signal is transferred back into the electrical domain by a photodiode. The signal is then electrically amplified and directly represents the input electrical modulating signal. The relation between the optical modulated signal power and the electrical signal power after detection is quadratic.

3.2 Multichannel analog communication

Existing AM CATV systems use *vestigial sideband* (VSB) to AM modulate the baseband television channel (see Fig. 3.2) onto an RF carrier. Furthermore, to be able to send multiple CATV channels,

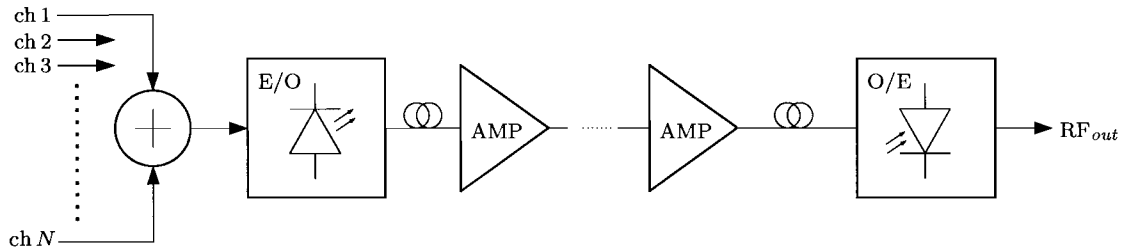

Figure 3.1: Schematic overview of an analog optical communication system using frequency division multiplexing

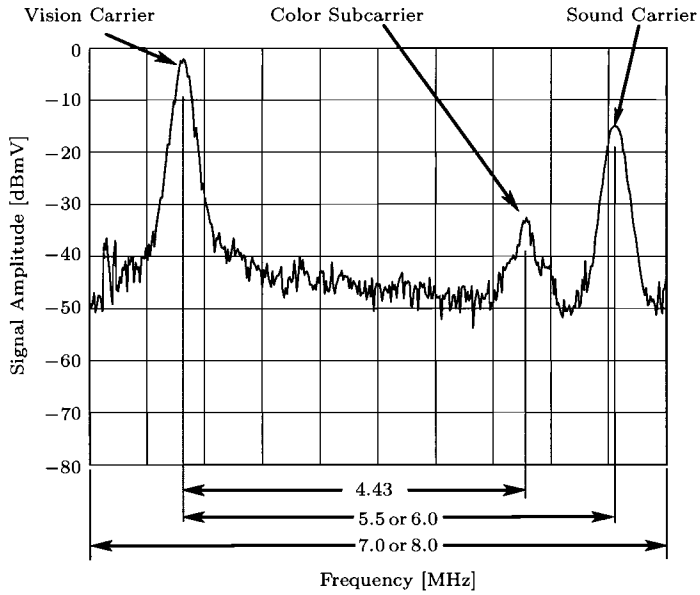

Figure 3.2: Frequency spectrum of a CATV channel, location of the sound and visual carriers. The FM modulated sound carrier is placed 5.5 or 6 MHz above the vision carrier and has a 100 kHz bandwidth.

a multiplexing technique called *frequency division multiplexing* (FDM) is used. In FDM, each channel is modulated on a different carrier frequency and these signals are then added together to form a single signal. With FDM it is not only important to ensure enough spacing exists between the channels to avoid interference, one should also guarantee sufficient linearity to avoid intermodulation distortion. The implications of this will be identified and detailed in the next sections.

Another term often used in multichannel analog communication is *subcarrier multiplexing* (SCM). AM-SCM is a method that not only uses FDM to multiplex several analog channels on one link, but also to multiplex digital QAM modulated channels. These digital channels can be used to transport DVB, HDTV and VoD digital streams. We will not go into the details of this type of digital multichannel communication, because analog CATV puts far more stringent requirements on the communication system in terms of noise, intermodulation and other nonlinear effects than QAM does for the digital signals. Recall Fig. 2.2 on page 11 for a typical CATV spectrum overview with both analog AM-VSB and digital QAM carriers. For the distribution of CATV channels over the frequency spectrum, as well as their channel bandwidth, there are several standards. The most

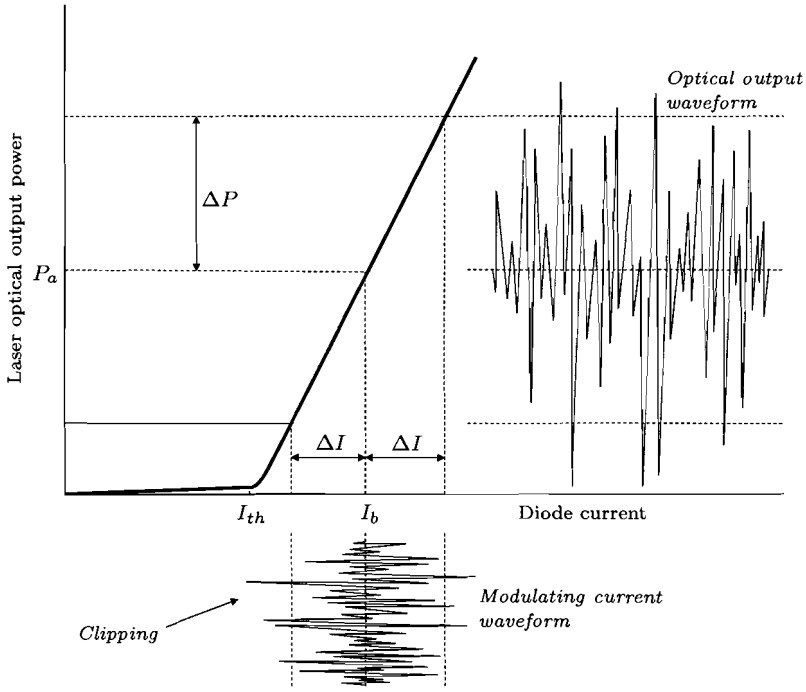

Figure 3.3: Direct modulation of the laser current: definition of the optical modulation index and laser clipping.

important of these so-called channel plans are the NTSC (used in the USA, Canada and Japan), SECAM (used in France and some Eastern European countries) and PAL (used in most of the rest of the world). Details on each of these channel plans are included in Appendix C.

A multichannel communication system is characterized by three important parameters: the carrier-to-noise ratio (CNR), the composite second order (CSO) and composite triple beat (CTB). The first one is largely dependent on the system power budget and the latter two are nonlinear intermodulation distortions. These parameters put stringent requirements on the optical analog communication system, especially on the laser diode and its driver electronics, because of the high signal levels to be handled. For this application, a distributed feedback (DFB) laser at either 1310 or 1550 nm has to be used. The laser will have to be highly linear to avoid nonlinear distortions and have a low relative intensity noise (RIN) to maintain a high CNR. At 1550 nm dispersion also plays a role. Optical pulse spreading caused by chromatic dispersion induces intermodulation distortions in the detector, leading to CSO. The design specifications for this kind of system are summarized as follows [2]: in terms of CNR, the modulation index has to be as high as possible to reduce the negative impact of laser RIN and receiver noise (shot noise and thermal noise). On the other hand, the modulation index is limited to reduce nonlinear distortions from laser clipping and intermodulation due to nonlinearities in the laser transfer function. Also, the laser diode DC bias current I_b should be optimized with respect to CSO [3], CTB and clipping noise. Finally, for directly modulated lasers a technique called predistortion or electronic distortion compensation is often used. This technique adds a compensating signal to the laser diode modulating current, based on the nonlinearities in the laser transfer function. This will result in lower nonlinear distortion in the optical signal [4]. For externally modulated lasers a similar linearization technique compensates for the nonlinear behavior of the (Mach Zehnder) modulator.

3.3 Carrier-to-noise ratio

One of the most important system parameters of any communication system is the signal-to-noise ratio for baseband signals or the equivalent carrier-to-noise ratio for modulated signals. This ratio is used as a qualitative measure of a system and can be used to easily compare the performance of different systems. In any communication system, there will be several unrelated sources of noise. In multichannel analog CATV transmission, the CNR consists of noise contributions from the shot noise, thermal noise, laser clipping noise, optical amplifier noise and relative intensity noise. The total system carrier-to-noise ratio (CNR) is the ratio of the carrier power and the addition of these unrelated noise contributions:

$$\mathrm{CNR} = \frac{C}{N_{shot} + N_{th} + N_{clip} + N_{ase} + N_{RIN}} \tag{3.1}$$

In this section, we will analyze these contributions and derive an expression for the total system CNR of an analog multichannel communication system.

We first derive an expression for the *optical modulation index* (OMI) from Fig. 3.3. The OMI (m_o) is defined as the ratio of half the peak-to-peak optical signal power and the average optical power, given by

$$m_o = \frac{P_{max} - P_{min}}{P_{max} + P_{min}} = \frac{\Delta P}{P_a} \tag{3.2}$$

where ΔP and P_a are defined in Fig. 3.3. The OMI for multichannel systems is usually given in percent modulation per channel.

If the laser is driven by a sinusoidal signal and the optical modulation index is defined as (3.2), the resulting output power will be

$$P_{\mathrm{opt}} = P_a(1 + m_o \sin(\omega t)) \tag{3.3}$$

which generates the following current in the linear regime of a *pin* photodiode

$$I(t) = I_p(1 + m_o \sin(\omega t)) \tag{3.4}$$

So the carrier signal power (in units of A^2) can be expressed as a function of the optical modulation index m_o and the photocurrent $I_p = \mathscr{R}\bar{P}$ (where $\mathscr{R}$ is the photodiode responsivity), by deriving the mean-square signal current from (3.4):

$$C = \langle i_{\mathrm{sig}}^2 \rangle = \frac{1}{2} m_o^2 I_p^2 \tag{3.5}$$

3.3.1 Photodetector noise

The noise generated by the photodetector can be divided into two parts: the noise generated by the photodiode itself and the thermal noise generated by the detector circuitry. For CATV applications, *pin* photodiodes are almost exclusively used, because of their high dynamic range, lower noise figure and lower reverse bias voltage requirements as compared to avalanche photodiodes (APDs). We will therefore assume a *pin* diode in our calculations and omit the photodiode gain parameter of an APD.

The photodiode noise consists of *shot noise* and dark-current noise, which are uncorrelated. Shot noise (sometimes also referred to as quantum noise) is a statistical Poisson process describing the generation of electrons by photons. The fluctuation in this Poisson process sets a fundamental limit on the sensitivity of the receiver. The dark-current is the current that flows from the photodiode when no light falls on the sensor. This current primarily originates from electrons and holes that

are generated by thermal effects on the p-n junction. The sum of the mean-square values of these currents is the photodetector noise component

$$\sigma_N^2 = 2q(I_p + I_D)B_e \tag{3.6}$$

where I_D is the photodiode dark current and B_e the receiver (electrical) bandwidth. Since the dark current is usually very small compared to the photocurrent, for practical applications the photodiode noise component reduces to

$$N_{shot} = 2qI_pB_e \tag{3.7}$$

The photodetector circuitry generates thermal noise. We will combine the input impedance of the preamplifier and the photodiode load resistance to form the equivalent photodetector resistance R_{eq}, which will generate a mean-square thermal Johnson noise current of

$$N_{th} = \langle i_{th}^2 \rangle B_e = \frac{4k_BT}{R_{eq}} F_t B_e \tag{3.8}$$

where k_B is Boltzmann's constant, T is the temperature and F_t is the noise factor of the preamplifier. The RMS value of the noise current, $\sqrt{\langle i_{th}^2 \rangle}$, is called the equivalent noise current density. This parameter is usually expressed in units of $\mathrm{pA}/\sqrt{\mathrm{Hz}}$, specifying the noise characteristics of a detector. For practical CATV applications, a detector with an equivalent noise current density of $< 8\,\mathrm{pA}/\sqrt{\mathrm{Hz}}$ is desirable, to not limit the system CNR, as we will see later on.

3.3.2 Laser clipping noise

When the laser output clips, i.e. $\Delta I > I_b - I_{th}$ (see Fig. 3.3), nonlinear distortion arises. This clipping distortion is known to be the fundamental limiting factor in multichannel CATV systems [5] and therefore there has been much theoretical research, leading to accurate models for the nonlinear clipping distortion [6]. From [7] we derive the nonlinear distortion from the mean and mean square of the nonlinear distortion current I_{NLD} as

$$\overline{I_{NLD}} = \frac{1}{\sqrt{2\pi}\sigma_s} \int_{-\infty}^{0} I \exp\left[-\frac{(I - I_b)^2}{2\sigma_s^2}\right] dI \tag{3.9}$$

and

$$\overline{I_{NLD}^2} = \frac{1}{\sqrt{2\pi}\sigma_s} \int_{-\infty}^{0} I^2 \exp\left[-\frac{(I - I_b)^2}{2\sigma_s^2}\right] dI \tag{3.10}$$

which will give the variance of the clipped current as

$$\sigma_d^2 = \overline{I_{NLD}^2} + \overline{I_{NLD}}^2 = I_p^2 \sqrt{\frac{2}{\pi}} \frac{\mu^5}{(1 + 6\mu^2)} \exp\left(\frac{-1}{2\mu^2}\right) \tag{3.11}$$

with μ the RMS optical modulation index, related to the per channel optical modulation index as $\mu = m_o\sqrt{N/2}$. This variance is related to the nonlinear distortion (again following [7]), which will give us an expression for the *carrier-to-nonlinear-distortion* ratio (using (3.5))

$$\frac{C}{NLD} = \frac{\mu^2 \frac{1}{N} I_p^2}{\Gamma \frac{1}{N} \sigma_d^2} \tag{3.12}$$

where the factor Γ represents the fraction of the distortion power which falls in the CATV band, which can be approximated by $\frac{1}{2}$. The 'trick' that is used in literature, is to define this nonlinear clipping distortion as a noise component. From (3.11) and (3.12), we get for the clipping noise (N_{clip})

$$N_{clip} = \frac{\Gamma I_p^2}{N} \sqrt{\frac{2}{\pi}} \frac{\mu^5}{(1 + 6\mu^2)} \exp\left(\frac{-1}{2\mu^2}\right) \tag{3.13}$$

3.3.3 Optical amplifier noise

If one or more optical amplifiers are present in the optical link, a noise contribution called *amplified spontaneous emission* (ASE) is introduced. This ASE beats with both the signal and itself, generating signal-spontaneous and spontaneous-spontaneous beat noise and an extra shot noise component at the photodetector. Expressions for these three noise components have been derived by Olsson [8], which for the signal-spontaneous beat noise leads to

$$N_{s\text{-}sp} = 4q\eta n_{sp}\frac{G-1}{G}I_pB_e \tag{3.14}$$

with η the optical amplifier quantum efficiency, G the optical gain and n_{sp} the population inversion factor. The population inversion factor is amongst others related to the geometry of the amplifying medium and is greater than, or in ideal cases equal to, one. It can be defined in terms of the birth and death rate of photons and a rule of thumb relates it to the optical amplifier noise figure as $F \approx 2n_{sp}$.

The spontaneous-spontaneous beat noise is defined as

$$N_{sp\text{-}sp} = q^2\eta n_{sp}^2\left(\frac{G-1}{G}\right)^2 B_e(2B_o - B_e) \tag{3.15}$$

where B_o is the optical bandwidth. It is important to notice that this noise component can be reduced by placing an optical filter before the photodetector to reduce the optical bandwidth B_o.

Amplified spontaneous emission also generates shot noise in the photodetector. This shot noise component is defined as

$$N_{shot\text{-}ase} = 4q^2\eta n_{sp}\frac{G-1}{G}B_oB_e \tag{3.16}$$

This ASE noise term is however very small compared to the other two ASE noise terms and the shot noise generated by the signal itself and is generally disregarded.

The amplifier (ASE) related noise components of the CNR are therefore

$$N_{ase} = N_{s\text{-}sp} + N_{sp\text{-}sp} \tag{3.17}$$

3.3.4 Relative intensity noise

The optical output power level of the laser diode will have very small random intensity fluctuations, which could for instance be caused by temperature variations or by spontaneous emission. The noise resulting from these random fluctuations is called *relative intensity noise* (RIN) and can be defined in terms of the mean-square intensity variations, because the random process is Poisson. First, we define the RIN as

$$\text{RIN} = \frac{\langle(\Delta P_L)^2\rangle}{\bar{P}_L^2} \tag{3.18}$$

where $\langle(\Delta P_L)^2\rangle$ is the mean-square intensity fluctuation of the laser output and $\bar{P}_L^2$ is the average laser light intensity. The RIN is defined in units of dB/Hz and for analog multichannel transmission, a laser with a RIN of -155 dB/Hz or better is required. If we assume that the RIN spectrum is flat over the bandwidth of interest, we can define the RIN noise power as

$$N_{RIN} = \sigma_{\text{RIN}}^2 = \text{RIN}\cdot I_p^2B_e \tag{3.19}$$

Apart from random intensity fluctuations, there are other effects that will influence the laser RIN value. An important property of RIN is that it is very sensitive to optical reflections in the system. These reflections, occurring from fiber splices or connectors, have to be kept as low as

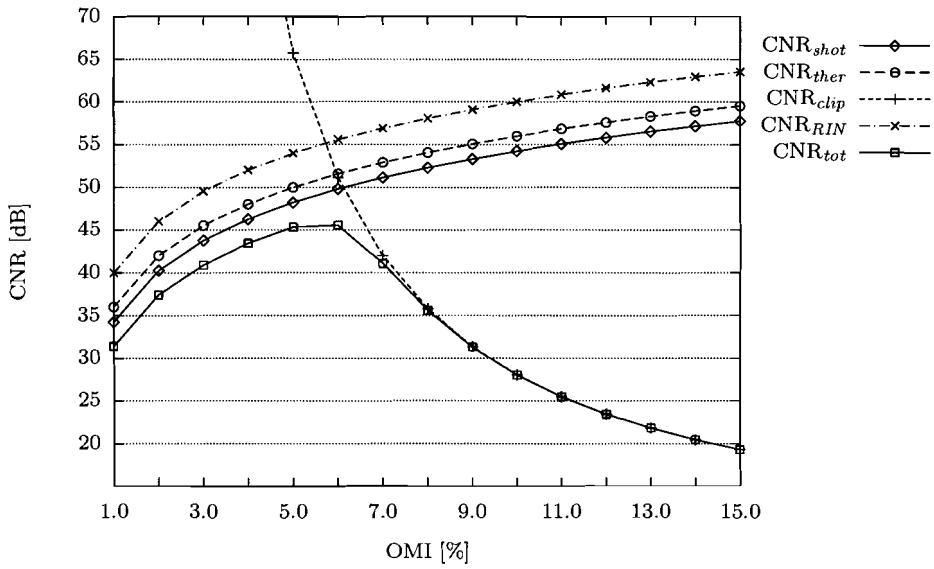

Figure 3.4: Theoretical plot of CNR contributions vs. OMI
Calculations using a directly modulated 1310 nm DFB laser diode with a RIN of −150 dB, a receiver with an effective noise current density of 4.5 pA/$\sqrt{Hz}$ and a responsivity of 0.85 mA/mW, −10 dBm received optical power and modulated with the CENELEC-42 channel plan.

possible. Therefore DFB lasers for CATV applications always include an optical isolator in the laser package, to reduce the influence of reflections. We define the *feedback power ratio* as

$$\text{FPR} = \eta_c^2 \alpha_f R \tag{3.20}$$

where η_c is the coupling efficiency of laser light into the fiber, α_f is the round-trip loss between the laser and the external reflection interface and R is the reflectivity of the external reflection interface. Way [9] has shown that this FPR for a DFB laser with optical isolator should be kept below −65 dB to stay close to intrinsic laser RIN values.

Double Rayleigh backscattering (DRB) is also known to have a negative effect on laser RIN values. Rayleigh backscatter is generated due to the interaction of the laser light with fiber refractive index inhomogeneities along the transmission path. This causes backscattering of part of the optical signal towards the source. When this backscattered signal is scattered a second time, this results in double Rayleigh backscatter which travels towards the receiver, where it generates interferometric noise with the main signal. For short distances up to 10 km the effect on the RIN is not significant however [10], so we will disregard DRB contributions to the laser noise.

3.3.5 Total carrier-to-noise ratio

All noise contributions derived above will degrade the carrier signal, so we can use them to define the system CNR (cf. (3.1)), which will yield

$$\text{CNR} = \frac{C}{N_{shot} + N_{th} + N_{clip} + N_{s\text{-}sp} + N_{sp\text{-}sp} + N_{RIN}} \tag{3.21}$$

This CNR is a very important quality measure for a multichannel system and signal requirements for the customer premises specified by [11] show that a minimum value of 46 dB for the CNR is needed for a good TV picture. Building a model to predict the behavior of a multichannel analog CATV system, the CNR is therefore one of the variables that will define the system requirements, as we will see in Chapter 5.

If we combine the theory in this section for a typical 1310 nm laser diode, we can analyze the impact of the different noise contributions to the total system CNR [12]. In Fig. 3.4 such a theoretical analysis is visualized in a plot of the different CNR contributions versus the optical modulation index. From this plot our earlier statement, the clipping noise being the fundamental limiting factor in analog multichannel communication, is immediately clear. Plots like these are a very good tool to analyze system performance and choose the optimal optical modulation index for operation.

3.4 Nonlinear distortions

Apart from the CNR, there are two nonlinear distortions that are used as a qualitative measure for the performance of a CATV system, CSO and CTB. In this section we will explore the theory that will explain where the CSO and CTB distortions come from. We will derive expressions for these composite distortions of second and third order, by looking at both classic intermodulation distortion and distortions specifically related to the optical communication system.

3.4.1 Harmonic distortions

In a multichannel system, the RF signal typically has more than 40 carriers, more or less equally spaced in the 50 to 900-MHz region. When these carriers pass nonlinear components like amplifiers, the laserdiode or photodiode, they will create mixing products, usually referred to as intermodulation products. Since some of these products will interfere with the main signal, this intermodulation is characterized as a distortion. In the following sections we will classify both second and third order intermodulation distortion (due to quadratic and third power nonlinear terms), which are largest when two respectively three carriers are interacting to generate distortion products. In multichannel systems, these distortions may become very large. Because of the regularity of the channel plan, several of these distortions will coincide at the same frequencies and add up power-wise to form so-called *composite distortions.*

Intermodulation is caused by nonlinearity of the system. Nonlinear elements can be characterized by a nonlinear transfer function as

$$e_0 = Ae_i + Be_i^2 + Ce_i^3 + \dots \tag{3.22}$$

where e_0 is the output voltage, e_i is the input voltage and A, B, C are gains. Using this formula, we will derive expressions for the first, second and third order distortions.

For a single sine wave input signal $e_i = E_i \sin(\omega t)$, the resulting output voltage when inserted into (3.22) will be

$$e_0 = A[E_i \sin(\omega t)] + B[E_i \sin(\omega t)]^2 + C[E_i \sin(\omega t)]^3 \tag{3.23}$$

Using trigonometric identities, this becomes

$$e_0 = \frac{BE_i^2}{2} + \frac{4AE_i + 3CE_i^3}{4}\sin(\omega t) - \frac{BE_i^2}{2}\cos(2\omega t) + \frac{CE_i^3}{4}\sin(3\omega t) \tag{3.24}$$

where the first term is a DC term, the second term is the desired signal, the third term is the second harmonic and the fourth term is the third harmonic. Normally we would use a low-pass or bandpass filter to reduce these undesired terms, but because we are interested in multichannel operation, this is not an option. In a multichannel system, some of these harmonics will fall inside the band and interfere with other channels, they are therefore referred to as *harmonic distortions.* We will disregard higher order harmonic distortions, because their amplitudes are significantly lower than the amplitudes of the lower order harmonic distortions and than the distortions we will discuss next.

Frequency	Ampl. squared
$3\omega_a$	0 dB
$\omega_a \pm 2\omega_b$	9.5 dB
$\omega_a \pm \omega_b \pm \omega_c$	15.5 dB

Table 3.1: Frequency components and amplitudes of third order distortion products

3.4.2 Second order distortion

For two sinusoidal input signals $e_i = E_i(\sin(\omega_1 t) + \sin(\omega_2 t))$, the resulting output voltage when inserted into (3.22) will be

$$e_0 = A[E_i(\sin(\omega_1 t) + \sin(\omega_2 t))] + B[E_i(\sin(\omega_1 t) + \sin(\omega_2 t))]^2 + C[E_i(\sin(\omega_1 t) + \sin(\omega_2 t))]^3 \quad (3.25)$$

The second order intermodulation distortions are generated by the quadratic term, which can be expanded using trigonometric identities (see also appendix A). The largest contributions to the second order distortion products are located at frequencies $\omega_a \pm \omega_b$.

In a multichannel system, these frequency components will largely fall inside the band and interfere with other channels. Given the channel plan, these distortion signals will have known frequencies. In most channel plans (like PAL, NTSC, CENELEC) the second order distortions are located 1.25 MHz below and above the video carrier, because they have equal channel spacing and the carrier frequency is located at $(n + 1.25)$ MHz. Several of these distortion products fall at the same locations, so we have to look at the sum. A measure for this composite distortion, the *composite second order* (CSO) distortion, is defined in Section 3.4.4.

3.4.3 Third order distortion

In order to calculate the dominant third order distortion products, we again analyze the respons of the system to a sinusoidal input signal. This time we use a signal that is comprised of three sinusoids, e.g. $e_i = E_i(\sin(\omega_1 t) + \sin(\omega_2 t) + \sin(\omega_3 t))$. Inserted into the nonlinear transfer function of (3.22), this will become

$$\begin{aligned} e_0 = {} & A[E_i(\sin(\omega_1 t) + \sin(\omega_2 t) + \sin(\omega_3 t))] + B[E_i(\sin(\omega_1 t) + \sin(\omega_2 t) + \sin(\omega_3 t))]^2 + \\ & + C[E_i(\sin(\omega_1 t) + \sin(\omega_2 t) + \sin(\omega_3 t))]^3 \end{aligned} \quad (3.26)$$

Using trigonometric identities on the third order term, we get a large expression containing the several harmonic and intermodulation frequency components of third order, which are displayed in Table 3.1, along with their relative amplitudes. From this table it becomes clear why only the $\omega_a \pm \omega_b \pm \omega_c$ frequencies are taken into account for the third order distortion: the square wave distortions at the $\omega_a \pm 2\omega_b$ frequencies are already 6 dB lower.

It would be interesting to know the relation between the desired signal and the distortions, but because the nonlinear model is different for each system, we cannot give relations between the A, B and C constants. We can only note that in normal systems, A will be much larger than B and C.

In a multichannel system, third order intermodulation generates a lot of distortion products that fall in band. Although third order distortions are normally smaller in amplitude, they outnumber second order distortions by far. As with second order distortions, their powers tend to accumulate at specific places in each channel, because of the regular channel spacing. The intermodulation will therefore generate composite distortion, measured by the *composite triple beat* (CTB), which is defined in Section 3.4.5.

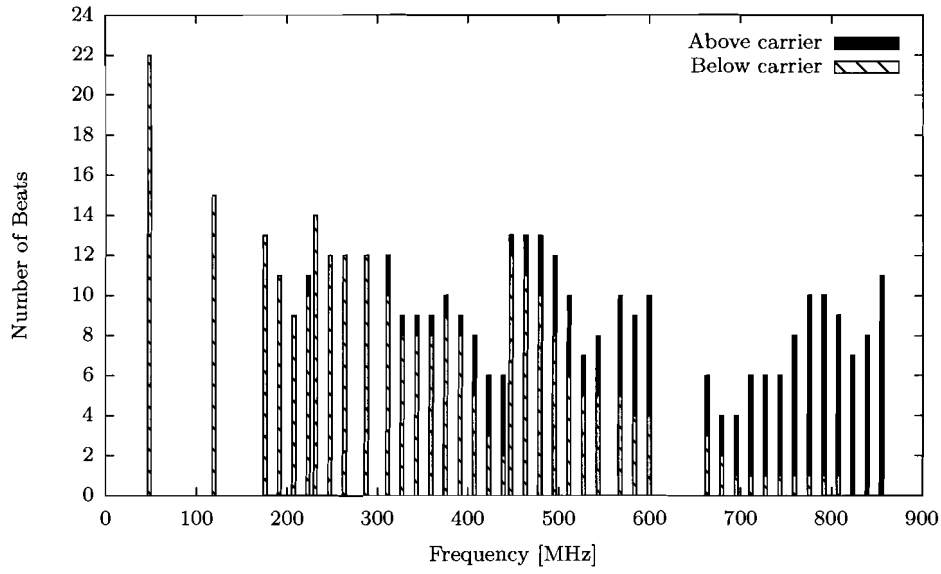

Figure 3.5: Number of CSO beats per channel in the CENELEC-42 channel plan

3.4.4 Composite second order

Composite second order (CSO) is defined as the sum of second order distortions on a given channel, or when a single value for an entire system is given, the worst-case (largest) sum of the power of these distortion products. CSO is usually expressed in dBc, decibels related to the carrier level. For CATV systems, CSO values of $-60\,\text{dBc}$ or better are typically required to ensure a good picture quality [13].

There are two contributions to CSO for an optical multichannel analog communication system. The classic contribution stems from second order intermodulation distortion, which was derived in Section 3.4.2. Using this distortion and the number of distortion products that fall in a particular channel, the frequency independent part of the CSO can be calculated. The other contribution is related to laser chirp and fiber dispersion.

The classic part of the CSO is defined as the sum of the power of the second order intermodulation products on a given channel ($\omega_a \pm \omega_b$, see also Fig. 3.6). We will therefore first need to find a definition for the amount of these distortion products and their distribution over the CATV band. A single distortion product is also called a *beat*. Using a small piece of software, it is possible to calculate the number of second order beats that will fall in band, given a channel plan and the number of channels N. Fig. 3.5 shows these beats for the CENELEC-42[1] channel plan. We can see that the maximum number of beats for the 42 CENELEC channels is 22 or 13.4 dB. For a more regular channel plan, like NTSC-79, the most dominant CSO products are located at the start and end of the band. This is also related to the distribution of the beats, as can be seen from the figures in Appendix B.

Using the worst-case number of beats per channel, we can estimate the system's worst-case CSO using the amplitude of the largest second order distortion component in that channel. Using this amplitude of the second order intermodulation IM_2, and the number of beats N_{beats}, we can calculate the theoretical worst-case CSO [14] as

$$\text{CSO} = (IM_2 - C)(\text{dB}) + 10\log(N_{\text{beats}}) \tag{3.27}$$

[1] CENELEC-42 is a European standard of 42 specifically selected PAL-B channels, ranging from 54 to 860 MHz, where the selection has been made to facilitate worst-case distortion measurements (see appendix C for a list).

where C is the carrier amplitude in decibels. More details on related measurement techniques for CSO will be discussed in Chapter 4.

For systems operating at 1550 nm, fiber dispersion combined with laser chirp can lead to CSO distortions, which come on top of the intermodulation related CSO generated by the preamplifier, laser diode, photodiode and postamplifier. Chirp is unwanted frequency modulation (FM) of the optical output signal of the laser. Chromatic dispersion will cause spreading of the optical signal: different wavelengths arriving at the photodiode at slightly different times. Even though we use only a single wavelength, laser intensity modulation will slightly change the output wavelength of the laser diode, causing wavelength variations (chirp). These slight wavelength variations, combined with chromatic dispersion, will introduce phase differences in the optical signal. After detection, these phase differences will translate into nonlinear distortions, primarily CSO [15].

Bergmann and Kuo [16] derived an extensive model for CSO, introducing dependencies on fiber chromatic dispersion, fiber span, channel frequency, laser chirp and optical modulation index. This model is very complex though and depends on specifications of the laser module that are not readily available. We will therefore use the more straightforward time-domain analysis of Yonetani [17].

$$\mathrm{CSO} = N_{beats}(\omega_1 + \omega_2)^2 z^2 \tag{3.28}$$

where z is

$$z = DL\frac{\lambda_c^2}{c}\eta_{\mathrm{FM}}(I_b - I_{th})m \tag{3.29}$$

and D is the chromatic dispersion (typically -17 ps/nm·km in single mode fiber at 1550 nm), L is the fiber length, η_{FM} is the FM response or chirp of the laser (typically around 100 MHz/mA))and λ_c is the laser center wavelength.

From this model it can be shown that the CSO will increase with increasing fiber span and increasing channel frequency. Also, the dependance on laser chirp is very important. In the case of direct modulation at 1550 nm, laser chirp will soon become the limiting factor. Much care must therefore be taken when designing a 1550-nm directly modulated laser module. The laser chirp will in that case severely limit the fiber span. In the case of external modulation however, the dispersion-induced CSO will reach intolerable levels only when the fiber span goes beyond approximately 10 km standard single mode fiber (SMF-28), for a 42-channel CATV system. Dispersion-induced CSO can be counteracted by using dispersion shifted fiber, but for our short distance applications this does not seem necessary. Laser chirp is the most important selection criterion for a 1550-nm directly modulated laser module.

3.4.5 Composite triple beat

Recalling our derivation of the third order intermodulation distortion of Section 3.4.3 at frequencies $\omega_a \pm \omega_b \pm \omega_c$, we now focus on the sum of the third order distortion components in a single channel, which we will define as the *composite triple beat* (CTB). For CATV systems, CTB values of -60 dBc or better are typically required for a good picture quality [13].

If we disregard the $\omega_a + \omega_b + \omega_c$ frequency component because in a normal system most of these fall out of band, there are three remaining terms of third order distortion. These terms will fall at $i + 0.25$ and $j + 0.75$, where $i, j \in [0, 8]$ for an 8 MHz PAL/CENELEC channel. Therefore in theory, 16 different CTB peak locations exist in an 8 MHz channel. Three of these locations are also plotted in Fig. 3.6, the rest is not shown to keep the figure readable. Appendix B shows the number of CTB beats per channel for both the CENELEC-42 and NTSC-79 channel plans. Here we can see that the channels in the middle of the CATV band have the largest contributions to CTB and the maximum number of beats for the CENELEC-42 channel plan is 319 or 25.0 dB. For NTSC-79 the maximum number of beats is 2,422 or 33.8 dB.

We can calculate the worst-case theoretical CTB using the third order intermodulation distortion IM_3 from Section 3.4.3. Using the maximum number of beats in the channel N_{beats} the following

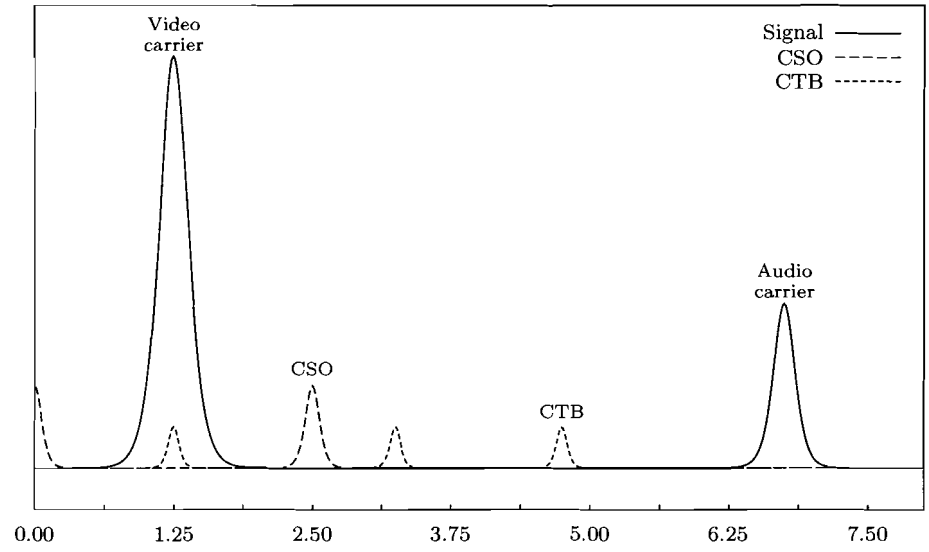

Figure 3.6: RF spectrum of a single CATV channel with second and third order distortion product locations

expression for the CTB [14] can be derived

$$\text{CTB} = (IM_3 - C)(\text{dB}) + 10\log(N_{\text{beats}}) \tag{3.30}$$

As with CSO, the CTB is often specified as a system parameter, meaning the worst-case CTB of all system channels. Measurement details for CTB can be found in Chapter 4.

3.4.6 Stimulated Brillouin Scattering

Another source for nonlinearity in optical fiber communication is caused by reflections, resulting from Stimulated Brillouin Scattering (SBS). In the optical fiber, the incident light will excite an acoustic wave when its power reaches a certain threshold. This acoustic wave alters the properties of the fiber, forming a refractive-index grating, on which the incident photons scatter and partially reflect. This process causes a nonlinear loss (attenuation), which is especially bad for 1550-nm amplified long-haul links. For continuous-wave (CW) light the SBS threshold P_{th} is given by [18]

$$P_{th,CW} = 21\frac{\zeta A_{\text{eff}}}{g_B L_{\text{eff}}}\frac{\Delta\nu_B \otimes \Delta\nu_L}{\Delta\nu_B} \tag{3.31}$$

where $\otimes$ denotes the convolution of the laser linewidth $\Delta\nu_L$ and the Brillouin bandwidth $\Delta\nu_B$; for Gaussian profiles, $\Delta\nu_B \otimes \Delta\nu_L = (\Delta\nu_B{}^2 + \Delta\nu_L{}^2)^{1/2}$. The polarization factor $\zeta = 2$ for random polarization state, A_{eff} is the effective core area of the fiber, g_B is the peak Brillouin gain coefficient ($= 4.6 \times 10^{-11}$m/W for silica fiber) and L_{eff} represents the effective interaction length, given by

$$L_{\text{eff}} = \frac{1 - \exp(-\alpha L)}{\alpha} \tag{3.32}$$

where α is the fiber attenuation coefficient and L the fiber length.

For systems that operate above the SBS threshold (both at 1310 and 1550 nm), SBS suppression will be needed. The most widely used method for SBS suppression uses wideband optical phase modulation (dithering) [19]. We will not go into the details of the suppression here, but refer to the literature on the subject [18, 19].

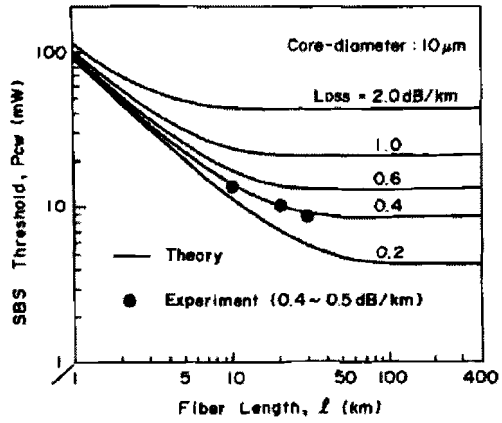

Figure 3.7: Dependence of SBS threshold for CW light on fiber length for several fiber losses (from [18]).

As we can see from (3.32) and Fig. 3.7 the SBS threshold is dependent on fiber length. For systems with a fiber length of up to 10 km, SBS effects on system performance are negligible. For a typical system with fiber length of more than 10 km however, the SBS threshold is as low as 6 dBm for 1550-nm and 9 dBm for 1310-nm systems. In such a case SBS suppression could be used to operate at powers above the SBS threshold. In point-to-point FTTH networks, high power signals are split in the central office before being launched into the residential fiber. This launched optical power will always be below the SBS threshold, especially because the fiber length is usually relatively short (< 10 km), so then no special SBS-combatting measures are needed.

Chapter 4

Measurements

In this chapter we will discuss the methods and the results of measurements that were carried out on two directly modulated 1310 nm CATV laser modules, which we will refer to as *Module A* and *Module B*. The modules both have a 75-Ohm RF input, no automatic gain control (AGC) and both have RF predistortion circuitry. *Module A* also has a RF pre-amplifier and therefore needs less input power and has a higher OMI in its linear operating range than *Module B*. In the operating range, the distortion (CSO, CTB) performance of the modules is optimized by predistortion for NTSC-110 operation and specified to be better than -62 dBc across their operating frequency (45-850 MHz). Detailed specifications for both modules are included in Appendix D.

The European Committee for Electrotechnical Standardization (CENELEC) has defined an European standard which details measuring methods for optical equipment in CATV networks [20]. The International Electrotechnical Commission (IEC) has defined a similar standard [21]. Most of the methods described below are taken from or inspired by these standards.

We will look at the key parameters for analog CATV transmission, as identified by the theory in the previous chapter. Optical modulation index, relative intensity noise, carrier-to-noise ratio and both two-tone and multi-tone measurements for second and third order distortions will be described and results for the two modules given. Some of the measurements from this chapter were conducted at the Eindhoven University of Technology and at BTI Bremi Elektrotechniek Eersel.

4.1 Optical modulation index

In Chapter 3 we have introduced the optical modulation index. We defined the OMI as the ratio of half the peak-to-peak optical signal power and the average optical power in (3.2). We can also define the OMI as a ratio of photodetector currents. For the linear region of the photodetector, the optical modulation index is equal to the electrical modulation index

$$m = \frac{i_{max} - i_{min}}{i_{max} + i_{min}} = \frac{\Delta i}{\bar{i}} \tag{4.1}$$

The average photocurrent $I_p = \bar{i}$ can be measured at the receiver using a current meter and Δi can be calculated from the output electrical power, which is measured using a spectrum analyzer or RF power meter. The OMI then becomes

$$m = \frac{\sqrt{2P_e/R_L}}{I_p} \times 100\% \tag{4.2}$$

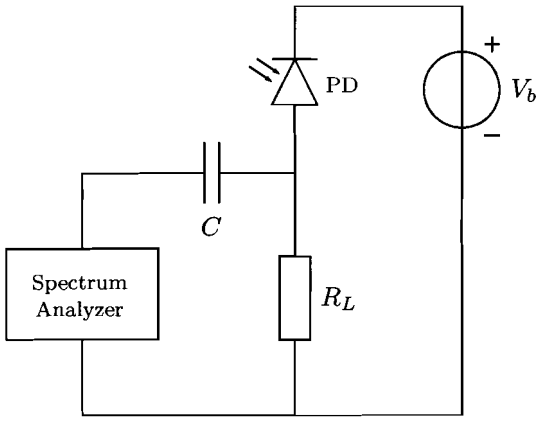

Figure 4.1: Receiver circuit to measure the optical modulation index

with R_L the photodetector load resistance, matched to the spectrum analyzer or power meter impedance (50Ωin our case). The corresponding measurement circuit is depicted in Fig. 4.1, with V_b the bias voltage for the photodetector (PD).

Measurements with this circuit conducted at Genexis, yield the graph in Fig. 4.2 for both *Module A* and *Module B*, plotting per channel RF input power versus OMI. For *Module A*, measurements at different bias currents were conducted. *Module B* has a fixed bias current. In order to validate the results (and because the results were not in agreement with the OMI values specified in the datasheets of the devices), another method of measurement of OMI was attempted. We tried to measure the OMI using an oscilloscope directly on the photodiode. This should yield a picture as provided with the OMI definition in Fig. 3.3 on page 17. We were however unable to measure the OMI this way, because the signal on the oscilloscope was very much distorted and the amplitude too low.

Because we suspected the matching of the spectrum analyzer to the load resistor to be the problem, the OMI measurements were also conducted at BTI Bremi, using their OMI measurement device, which was based on the same principle as Fig. 4.1 (see also OMI measurement details in [20]) but should provide better matching. These measurements yield the graph in Fig. 4.3 for both *Module A* and *B*, plotting per channel RF input power versus OMI. Comparing these results to those obtained at Genexis, we cannot explain the difference. The only possible cause for the large difference with the Genexis measurements could be the improper matching of the load resistance to the spectrum analyzer. Because this BTI Bremi device uses amplification and better separation between the photodetector and the spectrum analyzer, we have more faith in these measurements than the Genexis ones.

Still, the results are not in agreement with the manufacturers datasheet, which quote an OMI of 3.2% at 87.5 dBµV for *Module A* and an OMI of 2.9% at 98 dBµV for *Module B*. Because we have no other way to measure OMI directly, we will try using CNR curve fitting to come to more accurate results (see also [20]). The details of this method, that calculates OMI from theory fitted CNR measurements, are given in the CNR measurements section. As we will see, the results of this fitting are not in agreement with the values found here. No satisfying explanation has been found for this.

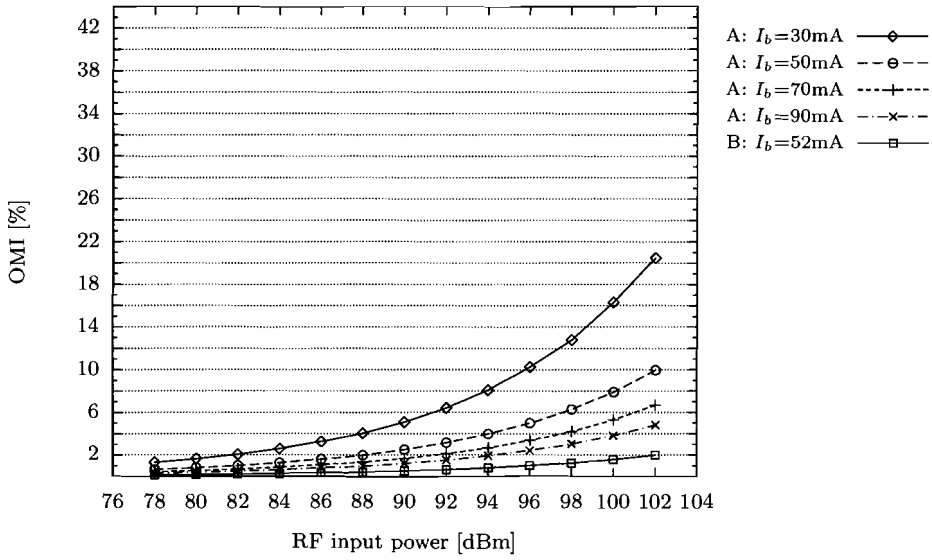

Figure 4.2: Measurements of per channel RF input power versus OMI for different bias currents of the two 1310-nm laser modules (A and B), conducted at Genexis.
$f = 100Hz$, $P_{opt,rec} = -1dBm$

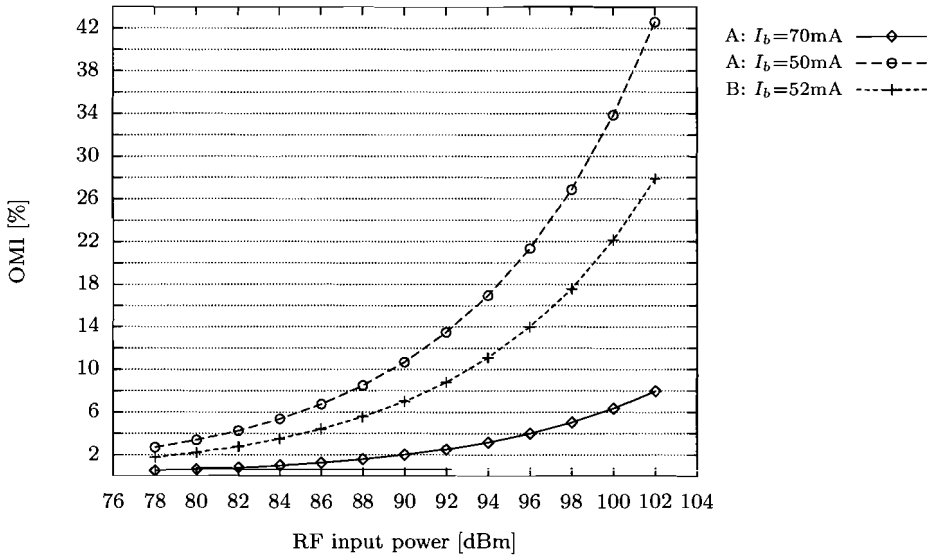

Figure 4.3: Measurements of per channel RF input power versus OMI for different bias currents of the two 1310-nm laser modules (A and B), conducted at BTI Bremi.
$f = 100Hz$, $P_{opt,rec} = -1dBm$

4.2 Relative intensity noise

The relative intensity noise cannot be measured directly, it is therefore calculated from a total system noise measurement [22], by subtracting the other contributions to the system noise. These contributions are, following from Chapter 3, the photodetector thermal noise and the shot noise. Because the RIN is defined as the relative noise in a bandwidth of 1 Hz, we will also define all other noise components within a 1 Hz bandwidth. We define the *system* RIN as

$$\mathrm{RIN}_{sys} = \frac{N_{tot}}{\bar{P}_o} = \frac{N_{RIN}}{\bar{P}_o} + \frac{N_{shot}}{\bar{P}_o} + \frac{N_{th}}{\bar{P}_o} \tag{4.3}$$

where $\bar{P}_o$ is the average received optical power and N_{RIN} is the laser RIN noise contribution. From (4.3) we can find the laser RIN as

$$\mathrm{RIN}_{laser} = \mathrm{RIN}_{sys} - \frac{N_{shot}}{\bar{P}_o} - \frac{N_{th}}{\bar{P}_o} \tag{4.4}$$

We can either use the system RIN marker function of the lightwave signal analyzer, or an electrical spectrum analyzer combined with a photodiode to measure the system RIN. Using the known properties of the photodetector and its amplifier (e.g. responsivity, load resistance and noise figures), we can calculate the laser RIN with (4.4).

Using a HP71400C Lightwave Signal Analyzer, the RIN of both laser modules (A and B) have been measured. This was done using the analyzer `RINsys` marker-function. The measurement procedure (using the system noise) as detailed above was used, using a thermal noise component of $N_{th} = -166\,\mathrm{dB/Hz}$ (noise figure of 8 dB) and a responsivity $\mathscr{R} = 0.8\,\mathrm{A/W}$[1]. Using a received optical power of 3 dBm, the resulting RIN values are more accurate, because at high optical powers the RIN dominates the system noise.

The following values are found for the maximum RIN, which is below the maximum threshold for good system performance. As we will see from the CNR measurements in the next section, these values are likely to be even better. We assume this is due to inaccurate values for the responsivity and noise figure of the analyzer, which were taken from the application note, but could not be verified.

A laser RIN performance of $\leq -160\,\mathrm{dB/Hz}$ could be expected for these modules, but the datasheets do not provide this information. The system RIN performance is therefore also examined in the CNR measurements of the next section.

Laser Module	RIN (max)
A	-155 dB/Hz
B	-156 dB/Hz

Table 4.1: RIN measurement results using HP71400C at $f = 300\mathrm{MHz}$, $P_{opt,rec} = -4\mathrm{dBm}$

4.3 Carrier-to-noise ratio

The measurement of the CNR itself is not a complicated task. The noise marker function of the HP8591E spectrum analyzer is used to determine the noise in a 1 Hz bandwidth and is then extended to the PAL noise bandwidth of 5 MHz. Using a set value for the per channel RF input power of the laser module (which results in a set value for the OMI), the setup in Fig. 4.6 is used to measure the system CNR of the laser module and the Genexis NTUO detector. For this CNR

[1]These values are taken from Agilent Product Note 71400-1: *'Measure Relative Intensity Noise'*

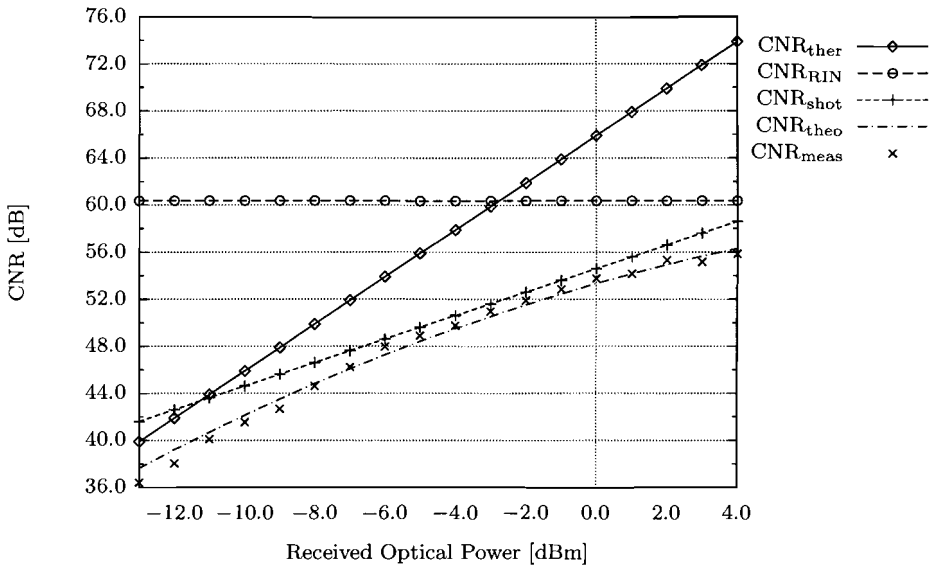

Figure 4.4: Measured CNR versus received optical power for *Module B*, fitted with theoretical values for CNR and its individual components.
Fitted values: $OMI \approx 3.3\%$, $\sqrt{\langle i_{th}^2 \rangle} = 4.5pA/\sqrt{Hz}$, $RIN = -160dB/Hz$; $P_{rf} = 101\,dB\mu V/ch$
Measured at: $f = 119.25MHz$, $P_{opt,laser} = 10.0dBm$

measurement only one signal generator is used. Because we want to assess the performance of the system, the received optical power is varied using an optical attenuator. This not only allows distinguishing between the individual contributions of the noise components, but also enables the assessment of system performance in terms of required minimum received optical power for an acceptable CNR value of 46 dB.

Fig. 4.4 plots the CNR (in dB) versus received optical power (in dBm) for laser module *B*. The measurements are fitted with the theory and the individual components of this theory are also plotted. This fit allows us to validate earlier measurements of OMI and RIN. It is important to note that the low values of the CNR (< 45 dB) were obtained by using a low noise (NF = 6dB) RF amplifier to elevate the system noise above the noise floor of the spectrum analyzer. The results that were obtained using the amplifier were compensated for the noise figure of the amplifier. Similar results for *Module A* are located in Appendix E.

Measurements of the CNR over the CATV frequency band are included in the two-tone measurements of the next section. This flatness over the CATV band is another important parameter for system design, because we have to specify the system performance for its worst channel. Related to this is the frequency response of the system. This response can be easily acquired with a network analyzer and the resulting frequency plot for *Module B* in combination with the NTUO receiver can be found in Fig. 4.5. Note that this measures the response of the combination of the laser module and the receiver. The result does not look very flat, but it is within what can be expected based on the specifications of both the laser module and the NTUO receiver (a flatness of ±1 dB across the CATV band).

4.4 Two-tone measurements

As we have seen in the previous chapter, an estimation of the CSO and CTB can be calculated from the second and third order intermodulation power. If we want to measure CSO and CTB,

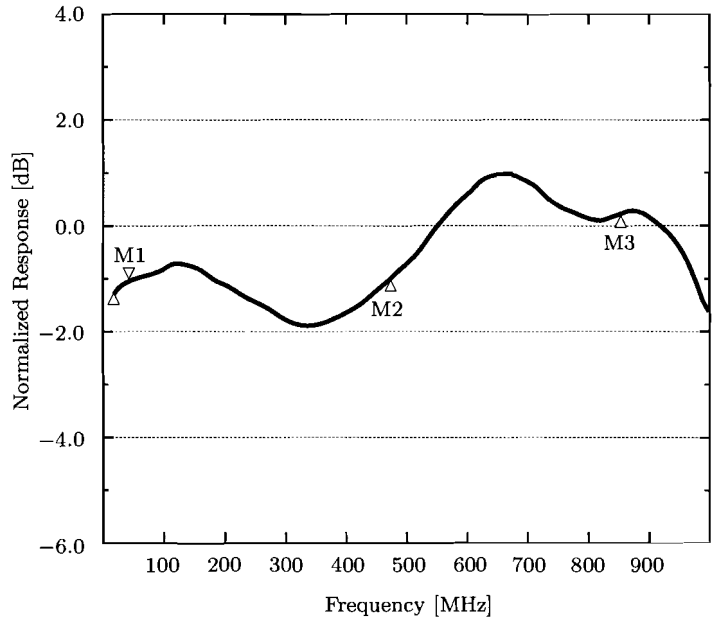

Figure 4.5: Frequency response of laser module B, in combination with the NTUO receiver, as measured with an HP 8753E.
The markers are positioned at the start, middle and end of the CATV band.

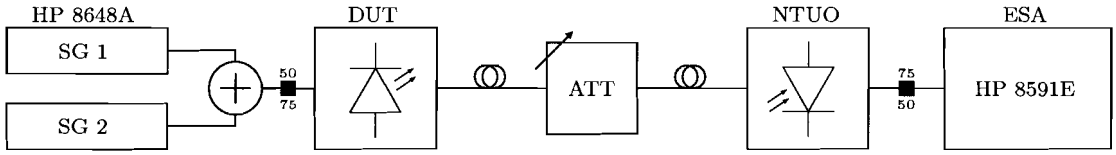

Figure 4.6: Two-tone measurement setup using two HP8648A signal generators, a Mini-Circuits ZFSC-2-4 power combiner, the laser module (Device Under Test), a variable optical attenuator, a NTUO receiver and a HP8591E electrical spectrum analyzer. Two minimum loss pads were used at the 50/75Ω and 75/50Ω transitions.

there are generally two ways to do so. In this section, we describe the simple method, based on two-tone measurements. In the next section, we will talk about using a multi-tone generator.

In a two-tone measurement, we combine two unmodulated carriers on different frequencies ω_1 and ω_2 using a power combiner and use this RF signal to directly modulate the laser. After optical attenuation and detection with the photodetector, we look at the output RF signal on the electrical spectrum analyzer. The output signal should now look something like Fig. 4.7, the two carrier signals at ω_1 and ω_2, two second order distortions at $\omega_2 - \omega_1$ and $\omega_1 + \omega_2$ and two third order distortions at $2\omega_1 - \omega_2$ and $2\omega_2 - \omega_1$. We now measure the difference between the carrier level and the distortion peaks. We will call this IMD_2 and IMD_3, the second and third order intermodulation distortion, in decibels related to the carrier level.

Since this method uses readily available measurement equipment it would be an ideal candidate for a simple indicative way of measuring CSO and CTB. It is our goal to match these 'simple' measurements to the more complex composite measurements, to be able to predict CSO and CTB performance. At the end of this section, we will look at the possibilities for this method.

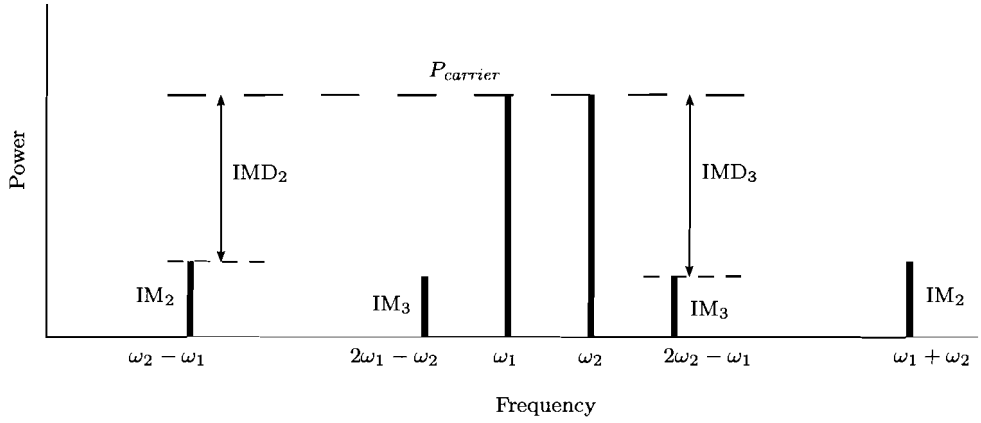

Figure 4.7: Second and third order intermodulation distortions in a two-tone measurement

4.4.1 Second order distortions

Recalling the theory of the previous chapter, we can directly use the second order intermodulation distortion IMD_2 in (3.27) and the number of beats, which depends on the frequency plan, to calculate CSO:

$$\text{CSO} = \text{IMD}_2 + 10\log(N_{\text{beats}}) \tag{4.5}$$

Trying to relate CSO to IMD_2 performance, several second order distortion measurements were conducted using the setup of Fig. 4.6. Both laser modules (A and B) showed very unstable second order distortion. Even with high values of video averaging on the spectrum analyzer, the amplitude variation of measurements over time was often as large as 3 dB. Therefore, we recorded a lower and upper bound for these averages and in turn took the average of those values. No explanation of this unstable behavior was found. Results of second order distortion versus OMI (RF input power per channel) for laser module A are given in Fig. 4.9. Alternatively, measurements on laser module B were conducted under varying frequency. These results are, together with similar results for third order distortion and CNR, plotted in Fig. 4.8.

4.4.2 Third order distortions

We can measure IMD_3 in the same way as IMD_2 and use a similar expression as in the previous section to relate this to CTB performance. However, we have to use a 'three-tone' measurement to get 'direct' third order distortions. The IMD_3 we identified in the two-tone setup is generated at $2\omega_1 - \omega_2$ and $2\omega_2 - \omega_1$ and is 6 dB lower than the predominant third order distortions that generate CTB (as can be seen from the expressions in Section 3.4.3). Compensating for this, it is however possible to calculate CTB using IMD_3 without the use of a third carrier:

$$\text{CTB} = \text{IMD}_3 + 6 + 10\log(N_{beats}) \tag{4.6}$$

The graph of Fig. 4.9 shows the third order intermodulation distortion of *Module A*, as measured with the two-tone setup. In the next section we will try to use these results to predict CSO and CTB performance of the system.

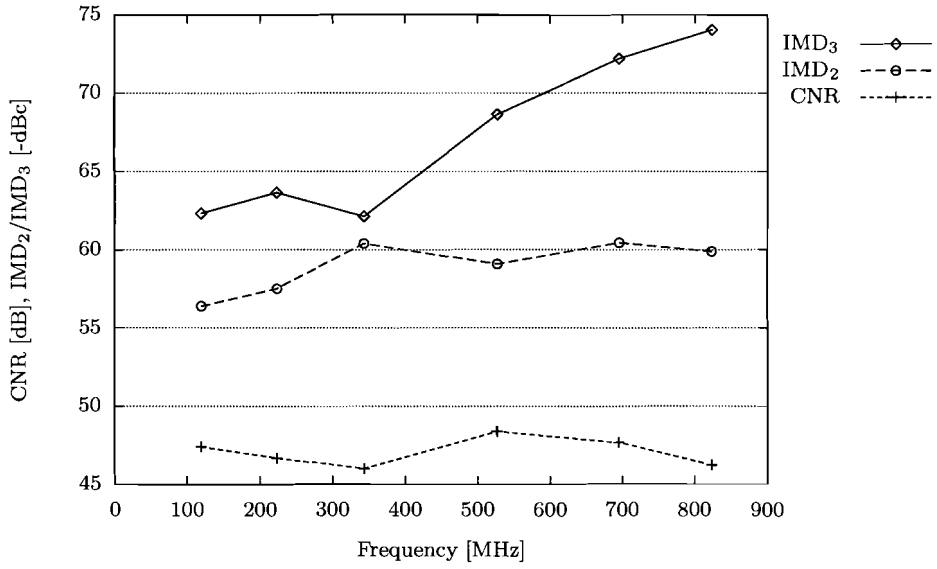

Figure 4.8: Two-tone measurement of the second and third order distortion and CNR over the CATV band, using *Module B.* $P_{opt} = -7dBm$, $P_{rf,in} = 101 dB\mu V/ch$
Measured distortion values with respect to carrier signal (dBc) were expected to be in the order of $-70dBc$ *for* IMD_2 *and* $-85dBc$ *for* IMD_3 *to be able to use them to theoretically predict CSO/CTB performance. See text for details.*

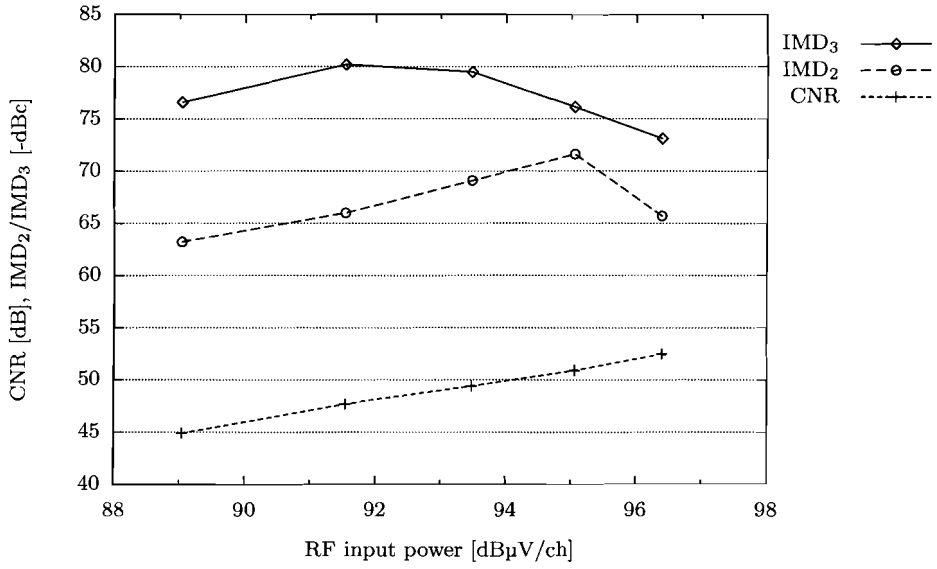

Figure 4.9: Two-tone measurement of the second and third order distortion and CNR versus per-channel RF input power, using *Module A.* $P_{opt} = -7dBm$, $f = 263.25MHz$
Previous fitting measurements suggest that these RF powers correspond with 3, 4, 5, 6 and 7% OMI, but this could not be directly measured. These measurements show that the per channel RF power should not exceed $92 dB\mu V$.

4.4.3 Composite distortions

Looking at the results from the second and third order distortion measurements, it should be clear that the values obtained with the 'simple' measurement setup will never translate into actual system CSO and CTB performance. The measured values of second and third order distortion (see Fig. 4.9) are already around the values expected for CSO and CTB. The compensation factor for the beats of CSO is around 10 dB, the factor for CTB is around 25 dB (values for CENELEC-42; factor is frequency dependent), so theoretically predicted CSO/CTB performance would be 10 to 25 dB lower than expected. In Appendix E graphs of CSO and IMD_2 and CTB and IMD_3 are given.

We will examine the cause for this discrepancy between measurements and theory. First, we will rule out the possibility that this behavior is caused by the measurement setup. Because the signal generators generate second and third order harmonics and the RF combiner generates second and third order distortions, this is a valid possibility. To be able to more accurately compare the multi-tone measurements of the next section and the two-tone measurements of this section, two channels of the multi-tone generator are used in a two-tone setup. This will enable us to exclude differences in measurement setup attributing to the discrepancy between expected results and actual measurements. Similar results were indeed obtained using the multi-tone generator in a two-tone setup and care was taken to eliminate all other potential sources of error in the setup (e.g. spectrum analyzer, receiver). The only possibility left is that this poor two-tone performance is caused by the laser module itself. It is most likely that the predistortion of the laser module, which is tuned for best CSO and CTB performance for a full CATV spectrum, actually worsens performance for small amounts of carriers. This is in fact the only viable explanation of the results of these two-tone measurements and it is therefore accepted. This means we found that it is not possible to predict CSO and CTB performance of a pre-distorted CATV laser module by using two-tone measurements. We will therefore focus on the multi-tone measurements of the next section.

4.5 Multi-tone measurements

A more realistic measurement technique than the two-tone measurement which better approaches reality is a multi-tone measurement (also referred to as Matrix measurement, after the manufacturer of a multi-tone measurement device). This measurement uses an array of highly linear signal generators which are tuned to match the channel plan, for instance 42 generators at the CENELEC-42 frequencies. The combined RF signal from the multi-tone generator is obviously a much more accurate approximation of the actual RF CATV spectrum than two carriers.

Using a bandpass filter to tune to a selected channel, we can easily use the spectrum analyzer to directly measure the composite second order distortion of the selected channel. Since CSO and CTB distortions fall at specific locations, they are easy to locate. Values are usually recorded for a few channels, in the lower, middle and upper part of the band to get an idea of their distribution over the CATV band. Fig. 4.10 shows how CSO and CTB are defined, in decibels related to the carrier level.

The following measurements where conducted with the BTI Bremi multi-tone generator, which has similar measurement capabilities as a commercial multichannel generator by Matrix Test Equipment Inc.. It consists of 42 signal generators, fixed at the 42 CENELEC specified frequencies (see Appendix C). The output power of these generators can be independently set over a 10 dB range with a maximum output power of 124 dBµV.

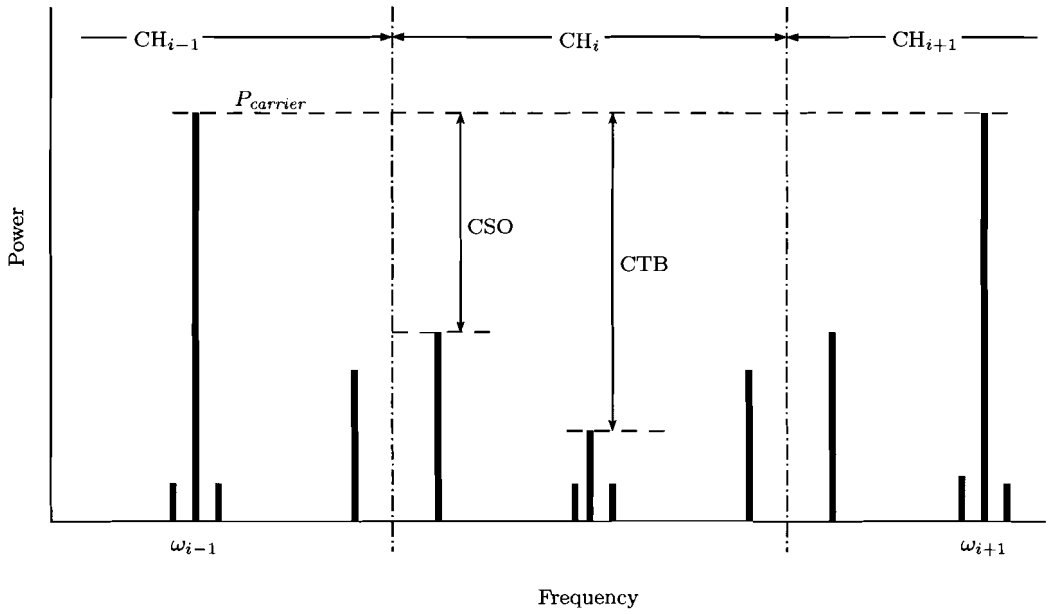

Figure 4.10: CSO and CTB measurement using a multi-tone generator

4.5.1 Composite distortions

At the start of a measurement, all 42 carriers have to be leveled, e.g. set to equal power. For the initial measurements, this level was set to 90 dBµV for *Module A* and 100 dBµV for *Module B*. These values are in the high end of the linear operating range, as to yield maximum OMI while keeping distortions low. For *Module B*, a low-noise hybrid 22 dB CATV amplifier was used to be able to provide 100 dBµV over the entire spectrum. The noise and distortion specifications of this amplifier were sufficiently good as to not influence the measurement.

The multi-tone measurement setup is detailed in Fig. 4.11. The optical power that is received by the NTUO photodetector can be set by using a variable optical attenuator. The amount of received optical power is a crucial parameter. Not only does the output power rise with a higher

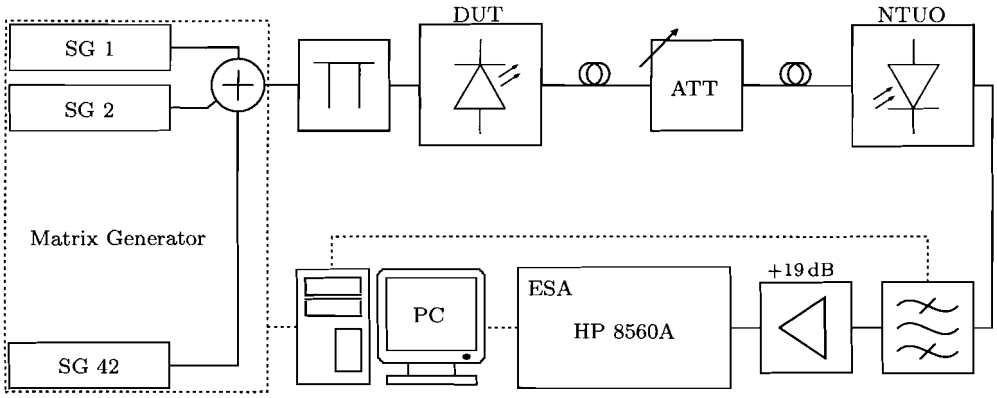

Figure 4.11: The multi-tone generator measurement setup is computer controlled using a Labview program.

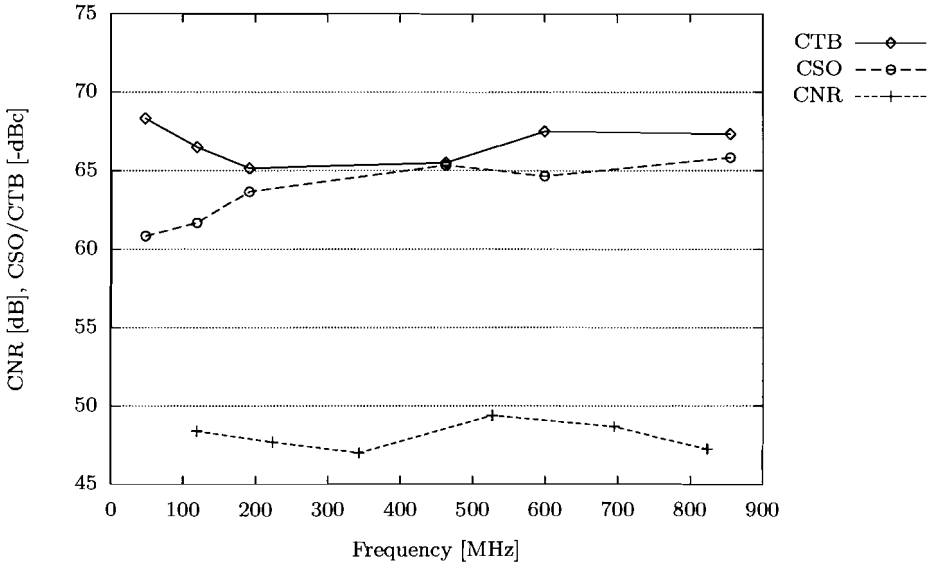

Figure 4.12: CSO, CTB and CNR over the CATV spectrum, measured using laser module B and the multi-tone generator. CSO and CTB values are in −dBc units to fit in one graph with CNR. $P_{opt} = -6dBm$, $P_{rf} = 100dB\mu V/ch$

optical power, we are also able to discriminate between laser module induced distortions (at low received optical powers) and receiver induced distortions (at high optical powers, e.g. receiver saturation).

At the output of the NTUO CATV receiver, a 19 dB hybrid CATV amplifier is needed to elevate the RF signal and noise levels above the spectrum analyzer noise floor. The noise and distortion of this amplifier are also low enough to not influence the measurement.

The automated measurement procedure measures the CSO and CTB at different locations across the spectrum. Results are displayed in Fig. 4.12 and seem to be in perfect agreement with the datasheet specifications (CSO < -62 dBc, CTB < -65 dBc, see Appendix D). It should be noted that the frequencies below 100 MHz are not used in a real CATV channel plan. The worse CSO performance at 48.25 MHz (c.f. Appendix B) is therefore not the bottleneck for the entire system.

A complication of measuring CTB with a multi-tone generator is that many of the CTB distortions fall at the same frequency as the carrier signal (recall Fig. 3.6). The carrier of the channel under measurement therefore has to be switched off.

Using the RF attenuator, we can measure the dependance of the nonlinear distortions on laser module RF input power. The results of these measurements are plotted in Fig. 4.13. Results for CSO and CTB for both modules (A and B) are plotted. Because the laser modules operate in different RF input power regions, the RF powers of *Module B* are on the primary x-axis and the RF powers of *Module A* on the secondary x-axis. From this figure, the maximum value for the RF input power for both modules can be derived, which helps us to find the optimal operating point for best overall system performance (high CNR and low distortions).

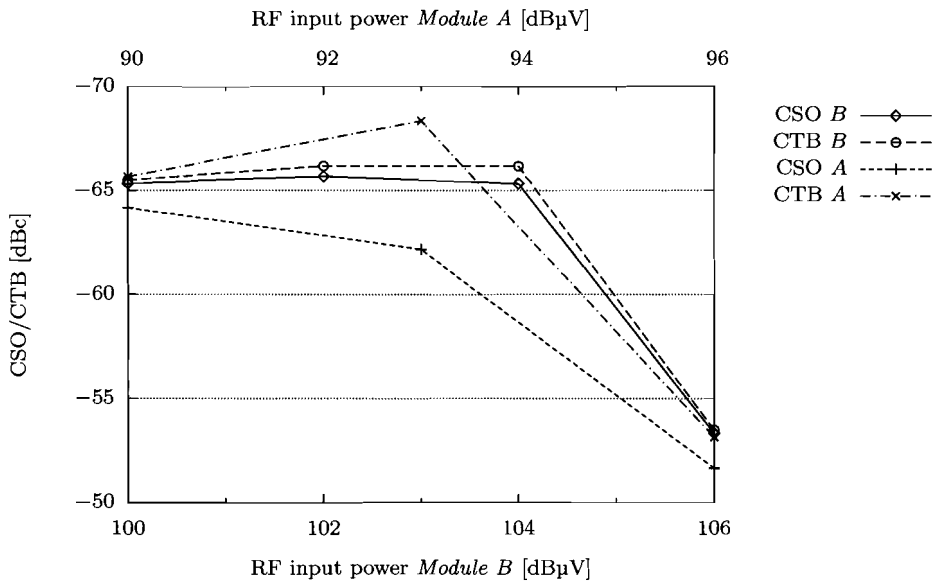

Figure 4.13: CSO and CTB versus input RF power for both laser modules.
$P_{opt} = -6dBm$, $f = 463.25MHz$

4.6 Conclusions

From the measurements conducted in this chapter, several conclusions can be reached. First of all, as we've seen, it is not possible to use the results of the relatively simple two-tone measurements to predict system CSO and CTB performance. We conclude that multi-tone measurements are a necessary tool to validate system performance. This contradicts our initial believes that we would be able to predict worst case CSO/CTB performance using two-tone measurements. As we've seen from the measurements, this discrepancy between theory and practice could be attributed to the laser predistortion, which is tuned for optimal multi-channel distortion performance. Because we have no details about how this predistortion operates, we cannot include its effects in our model. Another possible cause could be the frequency dependance of CSO and CTB, because if the CSO and CTB are very much frequency dependent, the theoretical extrapolation by multiplying with the number of intermodulation products does not work. This behavior is too complex to put into our model, as we have seen in Chapter 3.

We now conclude that with known RIN performance of the laser and known noise properties and detector responsivity of the receiver we can use a set OMI (RF input power) and the received optical power to model both CNR and CSO/CTB performance inside the operating range. Input for such a model is a CNR and CSO/CTB measurement conducted as described in this chapter. A model like this will be discussed in more detail in the next chapter.

As we have seen from the measurement results in this chapter, we have verified the vendor specified CSO and CTB, as well as the CNR performance of the two laser modules in a system measurement with the actual optical receiver to be used. The figures indicate that the so-formed system will have no trouble operating anywhere in the received optical power range between 0 and -8 dBm, when the per channel OMI and laser bias point are optimized. The RF input power per channel should be kept fixed, or automatic gain control (ACG) should be used in order to maintain a fixed RF modulating power (modulation index) for the laser however, which will result in a fixed OMI.

Chapter 5

System models

This chapter will describe different system topologies for the central office and present models that enable comparison of options on the basis of performance, necessary equipment and economical aspects.

5.1 Transmitter technology and network topology

In this section we will look at the four possible technologies for the CATV transmitter and the corresponding point-to-point network. We will introduce each technology briefly, sum up its key properties and look at the possibility to use this technology in a FTTH network.

5.1.1 1310-nm external modulation

External modulation for CATV transmission typically uses a $LiNbO_3$ Mach Zehnder Interferometer (MZI) modulator (which may have two complementary outputs) to modulate continuous wave laser light at 1310 nm generated by a semiconductor laser. Key properties of this combination of semiconductor laser and $LiNbO_3$ modulator at 1310 nm are low intensity noise (< -165 dB/Hz), narrow linewidth (< 10 kHz) and dual output power with typically 10 to 20 mW each (because of the relatively high insertion loss of the MZI). At 1310 nm there is however no commercially available optical amplification (only Semiconductor Optical Amplifiers (SOAs), or e.g. immature Nd-doped fiber amplifiers), so the link budget and transmission distance are limited. At 1310 nm fiber loss is 0.35–0.4 dB/km and fiber dispersion is near-zero, when using standard single-mode optical fiber (SMF-28).

1310-nm externally modulated CATV lasers are commercially available and are mostly used in medium-length point-to-point optical links in the optical trunk of HFC networks. They can also be used in FTTH networks, but the combination of high cost and limited link budget (split factor) due to modulator insertion loss and the absence of optical amplification makes this an economically unattractive option for distribution networks.

5.1.2 1310-nm direct modulation

As we have seen, 1310-nm direct modulation of a DFB laser bias current is also an option for optical CATV transmission. Linearity and intensity noise improvements of multi-quantum-well (MQW) DFB lasers and the use of pre-distortion has effectively made directly modulated lasers at 1310 nm as good as their externally modulated counterparts. Because directly modulated 1310-nm

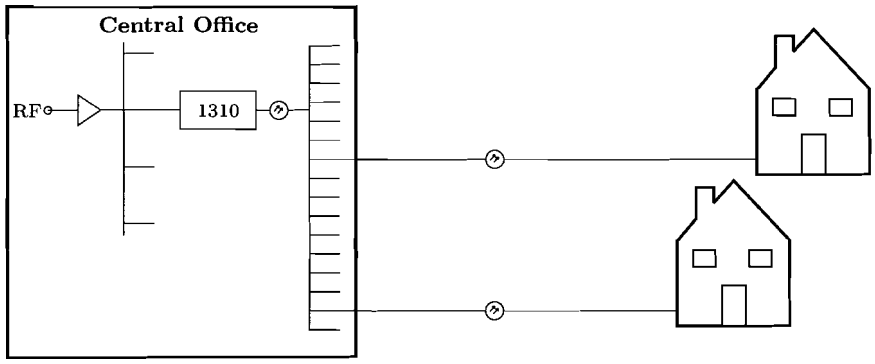

Figure 5.1: Central office configuration with 1310 nm laser: relatively small split directly after laser, because amplification is not possible. Multiple lasers will be needed to connect all subscribers.

DFB lasers are a lot cheaper, can have a higher output power and have good quality, they could be very attractive for use in FTTH systems.

The main disadvantage of this type of laser is again related to link budget. Because we cannot use amplification at 1310 nm, the output power of the laser (max. 30 mW) must be used for the entire link budget and the split factor will therefore be low (max. ca. 50), as we will see in our detailed analysis later in this chapter. A central office configuration based on a 1310-nm laser is schematically depicted in Fig. 5.1. As we can see this solution uses multiple CATV lasers and a RF tree of an amplifier and splitter to feed these lasers.

5.1.3 1550-nm external modulation

A 1550 nm MQW DFB laser can be externally modulated using a $LiNbO_3$ MZI intensity modulator, to create a CATV laser with an output power of 10–20 mW and low RIN (< -160 dB/Hz), which is typically amplified using Erbium-doped fiber amplifiers (EDFAs) to create a very high output power and thus a high link budget with high split factor. EDFAs do however have their own noise contributions (as we have seen in Chapter 3) and will generally degrade CNR performance with about 1 dB. Because of the external modulation, the frequency chirp of an externally modulated 1550-nm laser is very low, which results in low fiber dispersion penalties. At 1550 nm fiber loss is 0.2–0.3 dB/km and fiber dispersion ≈ 17 ps/nm/km, when using standard SMF-28 single-mode fiber.

This type of laser does however require suppression of SBS- and multiple-reflection-induced intensity noise and nonlinear distortions. In FTTH systems, a single laser can be used to provide thousands of households with analog CATV making use of EDFAs and splitters [23] to create a tree-shaped broadcast network (see Fig. 5.2). The cost of such a device is substantially higher than 1310-nm or directly modulated devices, as we will see later in the economical analysis.

5.1.4 1550-nm direct modulation

A directly modulated 1550-nm MQW DFB laser will exhibit similar RIN specifications as its externally modulated counterpart and have sufficient linearity for CATV transmission, but for a fraction of the cost. At first glance, this seems a good combination: low cost and upgradable power budget using EDFAs. Directly modulated DFB lasers have an inherent high chirp and associated nonlinear distortions resulting from fiber dispersion (dispersion induced CSO). This limits the reach of these directly modulated 1550-nm CATV lasers to only a few kilometers.

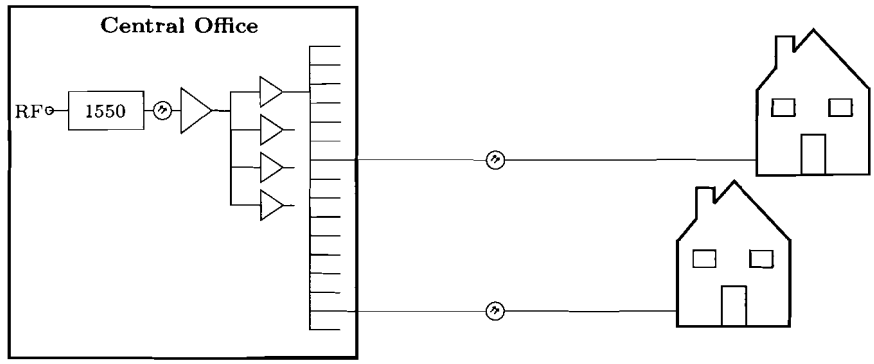

Figure 5.2: Central office configuration with 1550 nm laser: amplification with EDFAs and splitting allows tree-shaped network inside CO to achieve large split factors. All subscribers can share a single laser.

Recent developments made directly modulated 1550-nm CATV lasers interesting for use in longer optical CATV links. A commercial 1550-nm DFB laser was developed that is claimed to have a substantially lower chirp (35–45 MHz/mA compared to ~100 MHz/mA). Combined with predistortion, SBS suppression (16–17 dBm) and other electronic compensation techniques (which are not disclosed), commercial devices with reaches of 10 and 20 km are shipping and a 50-km version will be introduced very soon.

These directly modulated devices have a substantially lower cost, when compared to externally modulated devices. If the specifications of these lasers are indeed as promised, this technology is perfectly suitable for FTTH applications. Because Europe has relatively short distances between the subscribers home and the central office, the currently available 10-km units are ready for implementation in European FTTH networks now.

5.2 Technological analysis and equipment requirements

We have to keep in mind that we are looking for a scalable, low-cost implementation of analog CATV in FTTH, so we will examine CO equipment and a network topology that fits these constraints. Taking the observations of the previous section into account, as well as our measurements of the previous chapter, we will look at the two most interesting options in more detail: 1310-nm direct modulation and 1550-nm direct modulation optical analog CATV transmission.

5.2.1 1310-nm direct modulation

At 1310 nm dispersion induced distortions do not play an important role, because we operate in the near-zero dispersion window. Also, SBS suppression is not needed, because the optical signal will be split immediately and the launched power into the individual residential fibers will be well below the SBS threshold (see Chapter 3).

We will now do some calculations based on an example of a FTTH project connecting 1,000 homes with a maximum distance of 8 km to the central office. Most European towns and cities have an even lower distance to the central office, the larger cities in the Netherlands for example have a maximum distance to the central office of as low as 2 km. To be on the safe side for most common situations in Europe, 8 km will be a valid assumption. In this section we will only look at the

technological impacts and equipment requirements, an economical analysis will be given in the next section.

	Value	Unit
Operating wavelength	1310	nm
Optical output power	25	mW
Optical output power	14	dBm
Receiver optical power (min)	−8.0	dBm
Power budget	22.0	dB
Optical link length (max)	8	km
Fiber attenuation	0.2	dB/km
Splice and connector loss	1.2	dB
Optical link attenuation	2.8	dB
Splitting budget	19.2	dB
Splitting	32	×
Excess loss	3	dB
Optical splitting loss	15	dB
System margin	1.2	dB
Desired connections	1000	
Optical splitters	1 × 32	
RF splitter	1 × 32	
Realized connections	1024	

Table 5.1: Sample link budget calculation for 1310-nm solution

Table 5.1 calculates the link budget for this situation and shows the maximum achievable split ratio. We use a typical 25-mW 1310-nm DFB laser, which can meet CNR, CSO and CTB requirements at a received optical power of −8 dBm. As we can see from the figures in the table, a split factor per laser of 32 can be achieved in such a system. This means to connect 1,000 subscribers, we will need 32 laser modules and 32 of these 1 × 32 optical splitters. To connect the RF inputs of the laser modules, a 1 × 32 RF splitter and an appropriate (> 15 dB) RF CATV amplifier are needed. To be able to maintain a constant RF drive power for the CATV laser (and thus maintain a constant OMI), electronics for automatic gain control (AGC) have to be used, either as part of the laser module or as a separate circuit. The laser and optical splitting, combined with electronics for AGC, power supply and temperature control (if applicable) can be built in a 19" rack-mount box to create a single RF input, 32 optical output optical CATV transmitter. The needed equipment and its minimum specifications are summarized in Table 5.2. These calculations are done with a simple spreadsheet application, in which we can easily change values to see their impact on the link budget and required central office equipment.

Another model that was created analyzes the laser performance (in terms of CNR and CSO/CTB). It aims to calculate (using the theory we explored earlier) the behavior of the CNR, CSO and CTB given laser module and receiver specifications, laser module working point (bias current, OMI) and a single set of system measurements. This allows easy assessment of a laser module, as we can predict system performance (within operating ranges of receiver and transmitter) for different working points, with a single set of system measurements. Table 5.3 shows a sample output of the spreadsheet implementation of this model. This model also allows us to plot theoretical CNR behavior like we did in Fig. 3.4 on page 21 and predict CSO and CTB values over the operating range. We cannot take the operational performance of the predistortion into account, nor have we found an adequate model that fits our CSO/CTB measurements. The values of CSO and CTB this model calculates are therefore only an indication and a maximum threshold.

Equipment	Qt.	Specifications
1310 nm DM DFB laser module	32	$P_{out} = 22\,\text{mW}$, CNR= 46 dB, CSO/CTB= −60 dBc @ $P_{rec} = -8\,\text{dBm}$
1 × 32 optical splitter	32	Max. 3 dB additional insertion loss
1 × 32 RF splitter	1	
RF CATV amplifier	1	Gain > 15 dB, flat response, low noise (< −70 dBc)
Electronic Control Circuitry	1	Power supply, AGC, temperature
Rack-mount box and front-panel	1	

Table 5.2: List of equipment needed for the 1310-nm central office solution

Parameter	Set	New	
OMI	3	5	%
$P_{opt,las}$	13.4	13.4	dBm
$P_{opt,rec}$	−3.0	−1.0	dBm
CNR	53	54.7	dB
CSO	−64	−62	dBc
CTB	−69	−65	dBc

Table 5.3: Summary of the output of the laser performance model. Values for CNR, CSO and CTB were measured at the 'setpoint' and are calculated based on the new situation.

5.2.2 1550-nm direct modulation

Because of the network topology (immediate splitting in the central office, before launching into the residential fiber), SBS power thresholds are not expected to be reached in our FTTH implementation. Added to that is the fact that the new directly modulated 1550-nm DFB laser we have looked at in the previous section, has SBS suppression in the 16–17 dBm range, so we can safely disregards SBS. We will use standard commercially available EDFAs for amplification, which have a low (< 6 dB) noise figure so the CNR will not be affected too much. For typical models, a CNR degradation of max. 1 dB is specified. We will therefore target a higher received optical power at the receiver, to compensate for this.

We will now again do calculations based on the example of a FTTH project connecting 1,000 homes with a maximum distance of 8 km to the central office. This allows us to compare link budget and required central office equipment with the 1310-nm solution. In the next section we will compare these two solutions on a economical basis.

Because of the use of EDFAs, there are several different possibilities (e.g. different EDFA output powers) to achieve the desired split ratio. Table 5.4 calculates the link budget for two different situations and shows the maximum achievable split ratio. We use a 10-mW 1550-nm DFB laser, with CSO/CTB optimized for distances up to 10 km. In the first situation, the laser output is immediately split using a relatively low (1 × 8) split factor. This not only serves to increase total split factor (and thus possible connections), but also to lower the EDFA input power, which in turn lowers the EDFAs noise figure. After this initial split, 8 low-cost 23-dBm EDFAs are used to create a split factor of 1 × 128. This realizes 1,024 connections within the available power budget. The second solution, also summarized in Table 5.4, uses a single high power (32 dBm) EDFA to create a split factor of 1,024. Table 5.5 summarizes the equipment that is needed in the central office for both of these 1550-nm solutions. In the next section, we will compare the cost of

	Value (1)	Value (2)	Unit
Operating wavelength	1550		nm
Optical output power	10		mW
Optical output power	10		dBm
Initial splitting	8	1	×
Initial splitting loss	10	0	dB
EDFA input power	0.0	10	dBm
EDFA output power	23	32	dBm
Receiver optical power (min)	−6.0		dBm
Power budget	29.0	38.0	dB
Optical link length (max)	8		km
Fiber attenuation	0.4		dB/km
Splice and connector loss	1.2		dB
Optical link attenuation	4.4	4.4	dB
Splitting budget	24.6	33.6	dB
Splitting	128	1024	×
Excess loss	2		dB
Optical splitting loss	21.1	30.1	dB
System margin	1.5	1.5	dB
Desired connections	1000	1000	
Optical split level 1	1 × 8	–	
Optical split level 2	1 × 128	1 × 1024	
Realized connections	1024	1024	

Table 5.4: Sample link budget calculation for two 1550-nm solutions: (1) Using 8 low-cost, low-power EDFAs and (2) using 1 high-end, high-power EDFA.
Values unrelated to the EDFA-change are not repeated in column (2).

these two 1550-nm solutions and also compare it to the 1310-nm solution on the basis of cost per subscriber and scalability (which also has economical implications).

Equipment	Qt. (1)	Qt. (2)	Specifications
1550 nm DM DFB laser module	1	1	$P_{out} = 10\,\text{mW}$, CNR= 46 dB, CSO/CTB= −60 dBc @ $P_{rec} = -6\,\text{dBm}$, $l = 10\,\text{km}$
1 × 8 optical splitter (level 1)	1	–	Max. 1 dB insertion loss Rack-mount device
1 × 4 optical splitter (level 2)	8	–	Max. 1 dB insertion loss
1 × 32 optical splitter (level 2)	32	33	Max. 1 dB insertion loss
EDFA	8	1	*(1)* : $P_{opt,out} = 23\,\text{dBm}$, *(2)* : $P_{opt,out} = 32\,\text{dBm}$, Low noise figure (< 6 dB)

Table 5.5: List of equipment needed for the two 1550-nm central office solutions

5.3 Economical analysis

5.3.1 1310-nm direct modulation

The reason to look at 1310-nm direct modulation was mostly related to cost. We would like to be able to realize a solution that is both cost-effective and scalable. As we can see from the link budget calculation of the previous section, the proposed 1310-nm solution is highly scalable: we can connect subscribers in batches of 32. Because the RF splitting and amplification has considerably lower cost compared to optical splitting and amplification, we can maintain an almost fixed cost per subscriber no matter how many multiples of 32 we want to connect. We will now take a look at some indicative pricing information (based on various quotes) and calculate the cost of the 1,000 subscribers example of the previous section.

Qt.	Equipment	Unit Price	Total Cost
32	1310 nm DM DFB laser module	1,000	21,000
32	1 × 32 optical splitter	700	22,400
1	1 × 32 RF splitter	100	100
1	RF CATV amplifier	25	25
32	Electronics, rack-mount & assembly	1,000	32,000
		TOTAL:	**€ 86,525**
		Per Subscriber:	€ 85

Table 5.6: List of equipment cost for the 1310-nm central office solution. Pricing information is, although based on actual quotes, meant as an indication.

This translates into a cost of about 2,700 euro per 32 subscribers, or 85 euro per subscriber. As noted, subscribers are connected in batches of 32 which means that if less than 32 subscribers are connected, they share the cost of 2,700 euro. This level of scalability is the key advantage of this solution, combined with the low cost per subscriber.

5.3.2 1550-nm direct modulation

Direct modulation at 1550 nm is an attractive solution, because of the low cost of a directly modulated 1550-nm DFB laser and the possibility of using EDFAs. As we have seen in the previous section, there are several possibilities to realize the same split factor. Here we will compare the cost of the two different approaches we examined before, based on the example of connecting 1,000 homes. The comparison we will make here is not entirely accurate: because of the high cost of EDFAs we will compare a high-end commercial device for the single-EDFA-possibility with a number of low-cost EDFAs manufactured in China. We were unable to find a manufacturer for a comparable low-cost device that would be able to combine high output power (high split factor) with a low noise figure.

For the comparison with the 1310-nm directly modulated laser, it should be noted that optical splitter prices for the 1550-nm case are based on rack-mount devices, while the price of the optical splitters in the 1310-nm case are based on a quote of 'bare' waveguide splitters (with connectors). The reason for this difference is that in the 1310-nm case the splitters will be built in the same rack-mount box that also contains the laser. It might also be possible to build these 'bare' optical splitters inside the EDFA boxes, thus making the 1550-nm solution even less expensive.

As we can see, the single high-power EDFA solution realizes a lower cost per subscriber (82 euro) compared to the solution with more low-power EDFAs (104 euro). The scale factor of the high-power EDFA solution is however high: subscribers are connected in batches of 1,024. Compared to

Qt.	Equipment	Unit Price	Cost (1)	Cost (2)
1	1550 nm DM DFB laser module	2,100	2,100	2,100
8	EDFA 23 dBm	4,500	36,000	
1	EDFA 32 dBm	15,500		15,500
1	1 × 8 optical splitter	850	850	
8	1 × 4 optical splitter	440	3,520	
32	1 × 32 optical splitter	2,000	64,000	
33	1 × 32 optical splitter	2,000		66,000
		TOTAL:	**€ 106,470**	**€ 83,600**
		Per Subscriber:	€ 104	€ 82

Table 5.7: List of equipment cost for the two 1550-nm central office solutions. Pricing information is, although based on actual quotes, meant as an indication.

batches of 128 for the low-power EDFA case, this cannot be considered scalable. Either solution can however be interesting, based on the specific business case, initial subscriptions and expectations for future growth.

5.4 Conclusions

As we have seen in this chapter, direct modulation technologies are the most interesting for use in a cost-effective FTTH system. This is mostly related to their low cost (higher scalability) and comparable performance to their externally modulated counterparts. Heart of these two solutions are the 1310-nm directly modulated laser module and the 1550-nm directly modulated laser module.

When using a 1310-nm directly modulated device, we can realize a highly scalable and low-cost solution. It would be possible to build a rack-mount box that contains the CATV laser and optical splitters in a single housing. This device would have a single RF CATV input and 32 optical CATV outputs and it would be possible to build a CATV FTTH central office solution by just combining more of these boxes. Note that they each need a RF input signal, so for a group of boxes, a RF splitter and amplifier is needed. With such a device, the central office equipment will cost approximately 85 euro per subscriber, which is considerably less expensive than currently available externally modulated solutions. Added to that the fact that this solution can connect from 32 homes to thousands of homes for an almost constant price per subscriber, this solution offers both scalability and low-cost. It should be noted that there is some added complexity when the number of subscribers grows: each group of 32 connections (box) needs to be connected to the 'RF backbone', e.g. connected to a tree-shaped RF network transporting the AM-SCM signals. The cost of this RF equipment is however low compared to the optical equipment and the advantage of scalability is considerable. It should be noted though, that this RF network introduces additional noise and intermodulation distortions to the system and care should be taken to that the noise and distortions of the RF part of the network do not interfere with the optical performance.

Another possibility is the use of a 1550-nm directly modulated laser module. Recent technological advances have realized very low chirp 1550-nm DFB lasers, which can transport CATV signals over distances of 10 to 20 km, without the associated high dispersion induced distortions. Also, these modules are almost as low-priced as their 1310-nm counterparts. Their relatively low output power (10 mW) does however require the use of optical amplifiers (EDFAs) to be able to realize practical splitting ratio's. Connecting groups of 128 houses per EDFA was found to be both technically and economically possible, the cost per subscriber would be approximately the same as the 1310-nm

solution. An important advantage of using 1550 nm for CATV – apart from the ability to amplify – is that a single fiber solutions will be possible, as we will see in the next section.

Using the models for link budget and associated equipment requirements, a custom system design for a given situation (e.g. number of houses to connect) can also be made. For laser module selection procedures, the laser module performance model can be used to extrapolate laser performance in a system with three easy measurements, as we have seen from the theory of Chapter 3 and the model of Section 5.2.1.

Chapter 6

Single fiber FTTH

One of the important goals of the graduation project is the definition of a 'triplexer', a CPE that is able to provide triple-play services to the end-consumer using a single optical fiber into the residence. This single fiber solution poses several important technological challenges.

First of all, we will have to use different wavelengths for upstream data, downstream data and downstream analog CATV. Most commonly (like in APON, according to the ITU G.983 standards series), 1310 and 1490 nm are used for data, while 1550 nm is used for CATV. To avoid crosstalk of data on CATV and vice versa, the isolation of the filter (especially between 1490 and 1550 nm) needs to be very good. Because the CATV requirements for optical power level, CNR and distortions are very stringent (as we've seen before), data crosstalk on CATV poses the most difficult challenge. Schoop [24] has shown that a wavelength demultiplexer isolation of 30 dB or more is needed for data not to interfere with CATV.

Secondly, there is a challenge in the design of the electronics of the CPE. The analog CATV circuit is very sensitive to crosstalk and might pose EMC problems if mixed with the digital high speed data communication circuits. A modular approach, where these circuits are physically shielded and separated on different PCB's is therefore advantageous. The concept of a triplexer as a tri-directional small form factor pluggable (SFP) transceiver should therefore be questioned.

Lastly, a single fiber solution forces the CATV wavelength on 1550 nm. One of the reasons for looking at 1310 nm directly modulated laser modules for analog CATV transmission was that 1550 nm externally modulated CATV solutions are generally more expensive and less scalable. As we've seen in the previous chapter, it is however also possible to use new 1550 nm directly modulated laser modules for analog CATV transmission up to 20 kilometers. This lowers the cost price disadvantages of 1550 nm and opens the door to scalable, cost-efficient solutions. From a choice perspective, forcing 1550 nm for CATV transmission is however a disadvantage of a single fiber solution.

We will discuss two solutions to the technological problems above which use state-of-the-art optical components. One of these solutions resulted in the creation of a working demonstrator of both CPE and CO equipment, the other is still in a concept phase. For the discussion of 1310 vs. 1550 nm, we refer to the previous chapter.

Specific details on the technologies used to enable the single fiber solutions discussed in this chapter are located in Appendix F, which is released under embargo.

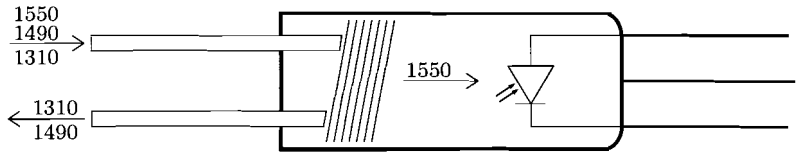

Figure 6.1: Schematic of the CATV detector with WDM edge filter.

6.1 CATV detector with data overlay

In order to preserve the advantages of the modular concept Genexis uses in its CPE, a special CATV photodetector is examined. This detector has two fibers: one incoming fiber and one outgoing fiber. On the incoming fiber, both 1310/1490 nm data and 1550 nm CATV are present. Before the actual detector a WDM edge filter is placed to reflect both 1310 and 1490 nm into the outgoing fiber and pass the 1550 nm CATV signal to the photodetector. A schematic of this device is shown in Fig. 6.1. The most important property is the isolation between the data and CATV signals. In our tests, it has proven impossible to generate a data distortion signal that would influence the performance of the CATV photodiode receiver.

For testing purposes and for building a system demonstrator, we have installed this special photodiode in a Genexis NTUO receiver. We have verified the performance of this receiver using CNR, CSO and CTB measurements. The performance is several decibels lower than the original detector, but still sufficient to demonstrate the concept.

To this extent, a system demonstrator, as schematically depicted in Fig. 6.2, is built using the modified NTUO and two data communication modules (OCG's) which have been fitted with new SFP 1310/1490 nm bidirectional 155 Mbit/s transceivers. The CPE side neatly fits into the Genexis *FiberXport* module, integrating the CATV and data modules with fiber management. For the CO side, a box is built which multiplexes an optical CATV signal with the 1310/1490 nm data signal generated by an OCG circuit. In this demonstrator, the multiplexing is done with a simple 3-dB splitter/combiner. In a real system, the power loss this splitter induces would not be acceptable and a real multiplexer with low insertion loss will have to be used. This is also a disadvantage of this system, because this multiplexer is a costly device and one is needed for each connection. The optical CATV signal is generated by a commercial 1554 nm laser, which is modulated by a VCR, which in turn gets a video signal from a DVD player. Here, the VCR is used as a modulator, to convert the RGB video stream from the DVD player into the AM-VSB signal needed to modulate the CATV laser.

6.2 Data BiDi with CATV overlay

In an effort to overcome the problem of the CO side of the single fiber system described in the previous section, we will now look at another device, which promises to keep the modular approach and fix the multiplexing problem.

This device is a 1310/1490 nm data transceiver with analog optical CATV overlay. This means that the device, just as the CATV detector, has an incoming and outgoing optical fiber and a reflective optical filter. In this case the reflective filter in the device reflects the 1550 nm CATV signal into the outgoing fiber, which is connected to the CATV receiver module. The data signals at 1310/1490 nm are left untouched and fed to the transceiver. Because there is both a TX1310/RX1490 and a TX1490/RX1310 device, a cost-effective, modular and transparant solution for both CPE and CO can be built using this device.

Comparing the data sheet specified values of the isolation, we can make some estimates of its performance and comparison to the CATV detector. The most important parameter is the isolation

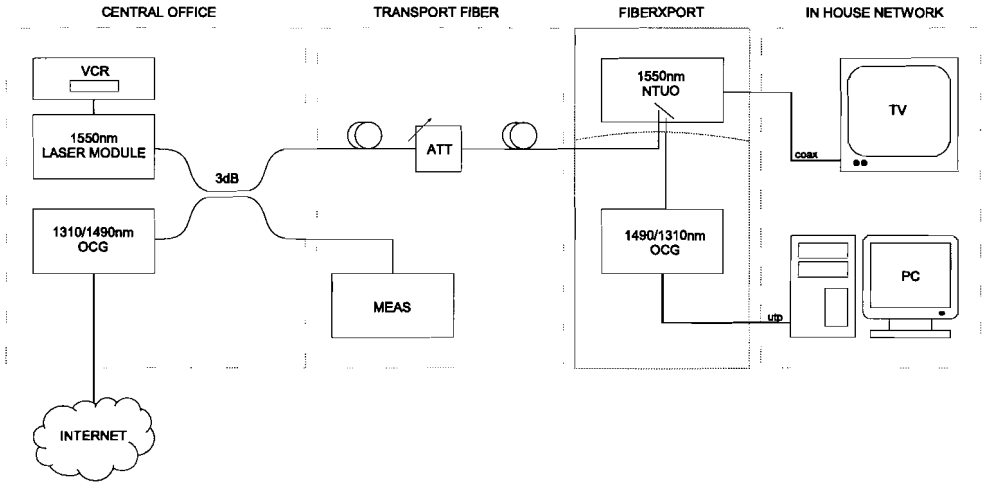

Figure 6.2: Single fiber demonstrator setup

between the CATV and data signal, mostly referred to as the crosstalk. This device promises a high optical isolation, which should be enough to match CATV requirements we have analyzed in the previous chapters.

Using this device, an optical ethernet switch with optical analog CATV overlay for use in the CO of a single fiber architecture becomes a viable possibility. It should be noted that this proposed switch also solves the missing CO solution when the reflective CATV detector for the CPE is used. This would mix the two single-fiber solutions and create both an easy to use modular CPE solution and a cost-effective and viable CO solution.

Chapter 7

Recommendations

To be able to answer our main research question – "*What technology enables low-cost, scalable CATV transmission in a point-to-point FTTH network?*" – we have first analyzed the validity of our theoretical model using measurements of the main system parameters CSO, CTB and CNR. As we were unable to relate the distortion results of relatively simple two-tone measurements to CSO and CTB, we conclude that multi-tone measurements are needed to analyze the CSO and CTB performance of the system, especially when using predistortion compensation to reduce the laser nonlinearity. We also conclude that the theoretical model of the CNR does relate well to our measurements.

Building on these measurements we have analyzed the possible technologies for the central office solution, both from a technological and from an economical perspective. We have concluded that there are two very promising candidates for the enabling technology for CATV in FTTH.

First of all there is the directly (intensity) modulated 1310-nm DFB laser transmitter. This device has a very low cost and is therefore interesting from a scalability point of view. It was shown that a single laser module could connect a maximum of 32 houses (because no amplification can be used) so if we combine this laser with optical splitting, we can build a 19" rack-mount box with a single RF input and 32 optical CATV outputs. The combination of multiple boxes like this creates a highly scalable central office solution, where the cost per subscriber is almost constant, regardless of the number of homes connected. This solution is however accompanied by an extensive electrical distribution backbone, with electrical power splitters and amplifiers, which may deteriorate a bit the noise performance and the intermodulation products.

Secondly, we have looked at a new product in the directly modulated 1550-nm category. As we have seen, dispersion induced distortions generally limit the transmission distance of such a laser to a few kilometers. This new product is claimed to have reduced laser chirp and improved predistortion to support transmission distances of 10 to 20 km over standard single mode fiber (SMF-28). Judging from the preliminary datasheet, we have deemed this a very interesting candidate for our low-cost, scalable technology. As we have seen, cost per subscriber will be approximately equal to the 1310-nm solution but scalability is not as high. This solution also has the reduced complexity of having just one laser with a single RF input and the use of 1550 nm as the wavelength of operation enables a solution where all triple-play services are WDM-multiplexed on a single fiber.

Concluding, the current technology of choice is the above described 32-port 1310-nm CATV box, because this solution is both highly cost-effective and scalable. It will allow the gradual roll-out of a FTTH project and the smooth migration from coaxial CATV distribution networks to optical access networks. It has both a robust technological basis and a promising business model.

As a related project, the feasibility of building a device for both central office and customer premises that enables the use of a single optical fiber is researched. On this single fiber, all three services (internet, telephony and CATV) should be multiplexed without interference to each other.

For this, WDM is used: ethernet data (both internet and VoIP) is transmitted on 1310 nm for upstream and 1490 nm for downstream, and analog CATV is transmitted downstream at 1550 nm. We have shown that technologies for both CPE and CO exist that enable this single fiber solution and we have verified the CPE side by building a system demonstrator and doing CATV-data and data-CATV interference measurements. We have also verified the performance of the enabling CATV receiver using the CNR, CSO and CTB measurements we have discussed before. For the CO we have proposed an architecture and technology for the implementation of a gigabit optical ethernet switch with optical analog CATV overlay.

For the future, research should focus on the 1550-nm directly modulated lasers with 10 km range. The promising specifications of such devices should be verified using similar system measurements as we have done for the 1310-nm case, with the addition of range-tests (e.g. verifying system performance over different lengths of SMF). In the analog CATV field of FTTH, traditional RF CATV knowledge needs to be combined with a good understanding of the theory of optical devices and phenomena to be able to come to solutions that go beyond the combination of standard building blocks, based on IEC- or CENELEC-proposed norms. Advancements in fundamental electro-optical design of lasers with favorable CATV properties enables system and network engineers to build a solution that realizes top-of-the-line performance with relatively low-cost equipment.

Appendix A

Second and third order distortion calculations

In order to calculate the second and third order distortion products, we analyze the response of the system to an input signal comprised of three sinusoids, e.g. $e_i = E_i(\sin(\omega_1 t) + \sin(\omega_2 t) + \sin(\omega_3 t))$. Inserted into the nonlinear transfer function of (3.22), this will become

$$\begin{aligned} e_0 = & A[E_i(\sin(\omega_1 t) + \sin(\omega_2 t) + \sin(\omega_3 t))] + \\ & + B[E_i(\sin(\omega_1 t) + \sin(\omega_2 t) + \sin(\omega_3 t))]^2 + \\ & + C[E_i(\sin(\omega_1 t) + \sin(\omega_2 t) + \sin(\omega_3 t))]^3 \end{aligned} \tag{A.1}$$

using trigonometric identities, we can expand this to

$$\begin{aligned} e_0 = & \frac{6BE_i^2}{4} + \frac{4AE_i + 15CE_i^3}{4}[\sin(\omega_1 t) + \sin(\omega_2 t) + \sin(\omega_3 t)] \\ & - \frac{2BE_i^2}{4}[\cos(2\omega_1 t) + \cos(2\omega_2 t) + \cos(2\omega_3 t)] \\ & + \frac{4BE_i^2}{4}[\cos((\omega_1 - \omega_2)t) - \cos((\omega_1 + \omega_2)t) + \cos((\omega_1 - \omega_3)t) - \\ & \quad - \cos((\omega_1 + \omega_3)t) + \cos((\omega_2 - \omega_3)t) - \cos((\omega_2 + \omega_3)t)] \\ & - \frac{3CE_i^3}{4}[\sin((\omega_1 \pm 2\omega_2)t) + \sin((\omega_1 \pm 2\omega_3)t) + \sin((\omega_2 \pm 2\omega_1)t) + \\ & \quad + \sin((\omega_2 \pm 2\omega_3)t) + \sin((\omega_3 \pm 2\omega_1)t) + \sin((\omega_3 \pm 2\omega_2)t)] \\ & + \frac{6CE_i^3}{4}[\sin((\omega_1 - \omega_2 + \omega_3)t) - \sin((\omega_1 - \omega_2 - \omega_3)t) - \\ & \quad - \sin((\omega_1 + \omega_2 + \omega_3)t) + \sin((\omega_1 + \omega_2 - \omega_3)t)] \\ & - \frac{CE_i^3}{4}[\sin(3\omega_1 t) + \sin(3\omega_2 t) + \sin(3\omega_3 t)] \end{aligned} \tag{A.2}$$

Here we recognize the terms which will make up CSO ($\omega_a \pm \omega_b$) and CTB ($\omega_a \pm \omega_b \pm \omega_c$), which are the largest products. These products also generally fall back in-band and near the carrier frequencies in equally spaced multichannel systems.

Appendix B

Calculating number of CSO and CTB beats

This appendix lists the results of the calculation of the number of beats for CSO and CTB, which was calculated using a piece of C++ software.

Both the CENELEC-42 and the NTSC-79 channel plans were used in this calculation.

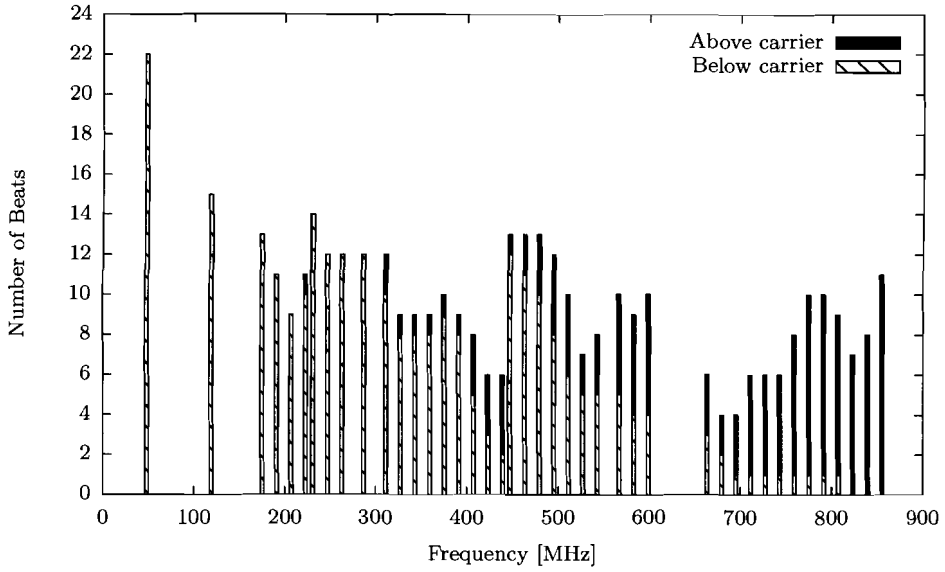

Figure B.1: Number of CSO beats in the CENELEC-42 channel plan

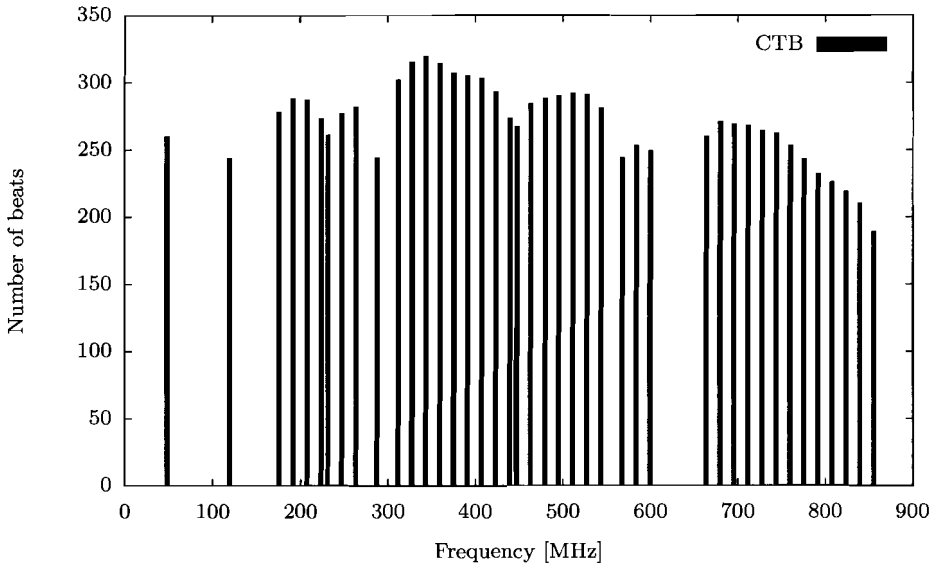

Figure B.2: Number of CTB beats in the CENELEC-42 channel plan

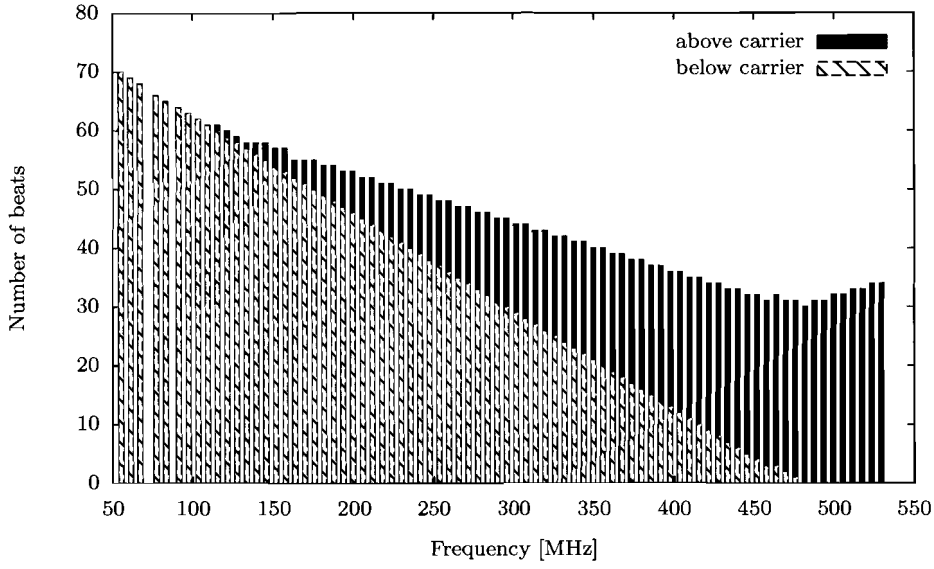

Figure B.3: Number of CSO beats in a NTSC-79 channel plan

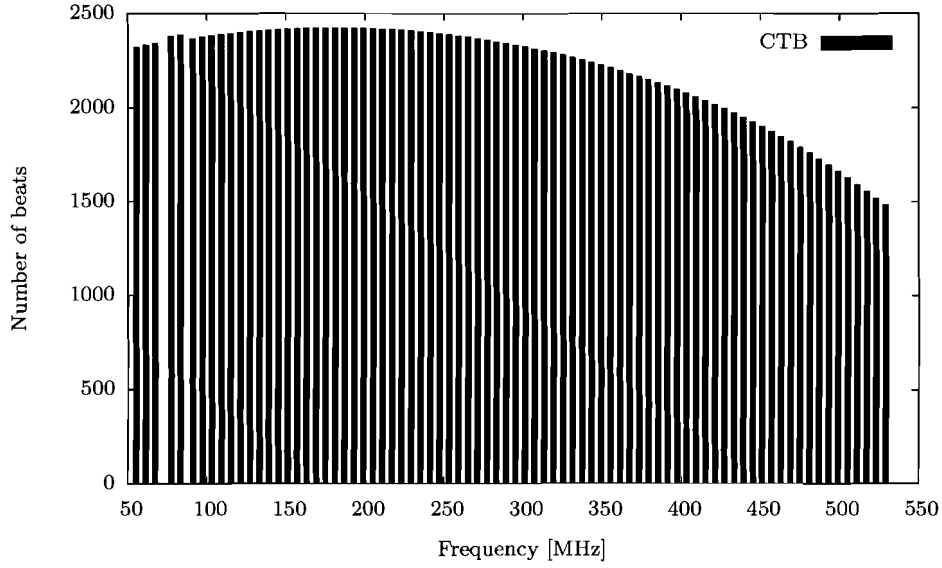

Figure B.4: Number of CTB beats in a NTSC-79 channel plan

Appendix C

Channel plans

This chapter lists the channel plans of the most important CATV standards in use in the world today, being NTSC, SECAM and PAL. It also lists the frequencies of the CENELEC-42 channel plan, which is used for CATV measurements and testing procedures.

C.1 CENELEC channel plan

TV Band	PAL #	Freq [MHz]
I	2	48.25
Midband	S3	119.25
III	5	175.25
		191.25
		207.25
		223.25
Superband	S11	231.25
		247.25
		263.25
	S19	287.25
Extended	S22	311.25
Superband	S24	327.25
	S26	343.25
	S28	359.25
	S30	375.25
	S32	391.25
	S34	407.25
	S36	423.25
	S38	439.25
	S39	447.25
	S41	463.25

TV Band	PAL #	Freq [MHz]
IV	22	479.25
	24	495.25
	26	511.25
	28	527.25
	30	543.25
	33	567.25
	35	583.25
	37	599.25
V	45	663.25
	47	679.25
	49	695.25
	51	711.25
	53	727.25
	55	743.25
	57	759.25
	59	775.25
	61	791.25
	63	807.25
	65	823.25
	67	839.25
	69	855.25

Table C.1: The CENELEC channel plan

C.2 PAL/SECAM channel plan

Ch #	Bandw [MHz]	Carrier [MHz]
E2	47.0-54.0	48.25
E3	54.0-61.0	55.25
E4	61.0-68.0	62.25
S3	118.0-125.0	119.25
S4	125.0-132.0	126.25
S5	132.0-139.0	133.25
S6	139.0-146.0	140.25
S7	146.0-153.0	147.25
S8	153.0-160.0	154.25
S9	160.0-167.0	161.25
S10	167.0-174.0	168.25
E5	174.0-181.0	175.25
E6	181.0-188.0	182.25
E7	188.0-195.0	189.25
E8	195.0-202.0	196.25
E9	202.0-209.0	203.25
E10	209.0-216.0	210.25
E11	216.0-223.0	217.25
E12	223.0-230.0	224.25
S11	230.0-237.0	231.25
S12	237.0-244.0	238.25
S13	244.0-251.0	245.25
S14	251.0-258.0	252.25
S15	258.0-265.0	259.25
S16	265.0-272.0	266.25
S17	272.0-279.0	273.25
S18	279.0-286.0	280.25
S19	286.0-293.0	287.25
S20	293.0-300.0	294.25
S21	302.0-310.0	303.25
S22	310.0-318.0	311.25
S23	318.0-326.0	319.25
S24	326.0-334.0	327.25
S25	334.0-342.0	335.25
S26	342.0-350.0	343.25
S27	350.0-358.0	351.25
S28	358.0-366.0	359.25
S29	366.0-374.0	367.25
S30	374.0-382.0	375.25
S31	382.0-390.0	383.25
S32	390.0-398.0	391.25
S33	398.0-406.0	399.25
S34	406.0-414.0	407.25
S35	414.0-422.0	415.25
S36	422.0-430.0	423.25
S37	430.0-438.0	431.25
S38	438.0-446.0	439.25
S39	446.0-454.0	447.25
S40	454.0-462.0	455.25

Ch #	Bandw [MHz]	Carrier [MHz]
S41	462.0-470.0	463.25
21	470.0-478.0	471.25
22	478.0-486.0	479.25
23	486.0-494.0	487.25
24	494.0-502.0	495.25
25	502.0-510.0	503.25
26	510.0-518.0	511.25
27	518.0-526.0	519.25
28	526.0-534.0	527.25
29	534.0-542.0	535.25
30	542.0-550.0	543.25
31	550.0-558.0	551.25
32	558.0-566.0	559.25
33	566.0-574.0	567.25
34	574.0-582.0	575.25
35	582.0-590.0	583.25
36	590.0-598.0	591.25
37	598.0-606.0	599.25
38	606.0-614.0	607.25
39	614.0-622.0	615.25
40	622.0-630.0	623.25
41	630.0-638.0	631.25
42	638.0-646.0	639.25
43	646.0-654.0	647.25
44	654.0-662.0	655.25
45	662.0-670.0	663.25
46	670.0-678.0	671.25
47	678.0-686.0	679.25
48	686.0-694.0	687.25
49	694.0-702.0	695.25
50	702.0-710.0	703.25
51	710.0-718.0	711.25
52	718.0-726.0	719.25
53	726.0-734.0	727.25
54	734.0-742.0	735.25
55	742.0-750.0	743.25
56	750.0-758.0	751.25
57	758.0-766.0	759.25
58	766.0-774.0	767.25
59	774.0-782.0	775.25
60	782.0-790.0	783.25
61	790.0-798.0	791.25
62	798.0-806.0	799.25
63	806.0-814.0	807.25
64	814.0-822.0	815.25
65	822.0-830.0	823.25
66	830.0-838.0	831.25
67	838.0-846.0	839.25
68	846.0-854.0	847.25

Table C.2: The PAL/SECAM channel plan

C.3 NTSC channel plan

Ch #	Bandw [MHz]	Carrier [MHz]
2	54.0-60.0	55.25
3	60.0-66.0	61.25
4	66.0-72.0	67.25
5	76.0-82.0	77.25
6	82.0-88.0	83.25
FM	*88.0-108.0*	
95	90.0-96.0	91.25
96	96.0-102.0	97.25
97	102.0-108.0	103.25
98	108.0-114.0	109.25
99	114.0-120.0	115.25
14	120.0-126.0	121.25
15	126.0-132.0	127.25
16	132.0-138.0	133.25
17	138.0-144.0	139.25
18	144.0-150.0	145.25
19	150.0-156.0	151.25
20	156.0-162.0	157.25
21	162.0-168.0	163.25
22	168.0-174.0	169.25
7	174.0-180.0	175.25
8	180.0-186.0	181.25
9	186.0-192.0	187.25
10	192.0-198.0	193.25
11	198.0-204.0	199.25
12	204.0-210.0	205.25
13	210.0-216.0	211.25
23	216.0-222.0	217.25
24	222.0-228.0	223.25
25	228.0-234.0	229.25
26	234.0-240.0	235.25
27	240.0-246.0	241.25
28	246.0-252.0	247.25
29	252.0-258.0	253.25
30	258.0-264.0	259.25
31	264.0-270.0	265.25
32	270.0-276.0	271.25
33	276.0-282.0	277.25
34	282.0-288.0	283.25
35	288.0-294.0	289.25
36	294.0-300.0	295.25
37	300.0-306.0	301.25
38	306.0-312.0	307.25
39	312.0-318.0	313.25
40	318.0-324.0	319.25

Ch #	Bandw [MHz]	Carrier [MHz]
41	324.0-330.0	325.25
42	330.0-336.0	331.25
43	336.0-342.0	337.25
44	342.0-348.0	343.25
45	348.0-354.0	349.25
46	354.0-360.0	355.25
47	360.0-366.0	361.25
48	366.0-372.0	367.25
49	372.0-378.0	373.25
50	378.0-384.0	379.25
51	384.0-390.0	385.25
52	390.0-396.0	391.25
53	396.0-402.0	397.25
54	402.0-408.0	403.25
55	408.0-414.0	409.25
56	414.0-420.0	415.25
57	420.0-426.0	421.25
58	426.0-432.0	427.25
59	432.0-438.0	433.25
60	438.0-444.0	439.25
61	444.0-450.0	445.25
62	450.0-456.0	451.25
63	456.0-462.0	457.25
64	462.0-468.0	463.25
65	468.0-474.0	469.25
66	474.0-480.0	475.25
67	480.0-486.0	481.25
68	486.0-492.0	487.25
69	492.0-498.0	493.25
70	498.0-504.0	499.25
71	504.0-510.0	505.25
72	510.0-516.0	511.25
73	516.0-522.0	517.25
74	522.0-528.0	523.25
75	528.0-534.0	529.25
76	534.0-540.0	535.25
77	540.0-546.0	541.25
78	546.0-552.0	547.25
79	552.0-558.0	553.25
80	558.0-564.0	559.25
81	564.0-570.0	565.25
82	570.0-576.0	571.25
83	576.0-582.0	577.25
84	582.0-588.0	583.25
85	588.0-594.0	589.25

Table C.3: The NTSC channel plan

Appendix D

Laser module datasheets

This appendix will list tables of specifications from the datasheets of the laser modules used in this project. All these values are given by the manufacturer, we have conducted our own measurements to verify system performance.

D.1 Laser module A

Below are the datasheet specifications and the specific manufacturer test results of the 1310-nm laser module *A* used for the measurements in this project.

D.1.1 Absolute Maximum Ratings

Parameter	Symbol	Condition	Min	Max	Unit
Operating Temperature	T_c	$I = I_{op}$	−20	65	°C
Storage Temperature	T_{stg}	–	−40	70	°C
Laser Forward Current	I_f	–	–	120	mA
Laser Reverse Bias	V_r	–	–	2	V
Photodiode Reverse Bias	V_{rpd}	–	–	10	V
TEC Current	I_{tec}	$-20°C < T_c < +65°C$, $T_{op} = 25°C$ $I_f = 100mA$		1.5	A

D.1.2 Electrical and optical characteristics

Parameters are over operating temperature range unless otherwise noted.

Parameter	Symbol	Test Conditions	Min	Typ	Max	Unit
Center Wavelength	λ_c	CW	1300	1310	1320	nm
Spectral Width (−20 dB)	$\Delta\lambda$	CW	–	0.1	1.0	nm
Optical Output Power	P_o	CW, $T_L = 25$°C	6	–	31	mW
Optical Isolation	I_S	$T = 25$°C	30	–	–	dB
Side-mode Suppression Ratio	SMSR	CW	30	–	–	dB
Threshold Current	I_{th}	$T_L = 25$°C	–	12	18	mA
Operating Current	I_{op}	CW	–	–	90	mA
Forward Voltage	V_F	CW	–	1.2	1.7	V
Monitor Current	I_{mon}	$V_{rpd} = 5$ V	10	–	150	μA/mW
Monitor Dark Current	I_D	$V_{rpd} = 5$ V	–	–	200	nA
Operating Temperature	T		−20	–	65	°C
Tracking Error	γ	I_{mon} =const, $\gamma = 10\log(P_o/P_r)$ [dB]	−0.5	–	0.5	dB
Thermistor Resistance	R_t	$T = 25$°C	9.5	–	10.5	KΩ
Thermistor B Constant	B	$T = 25$°C	–	3900	–	K
TEC Current	I_C	$\Delta T = 40$°C	–	–	1.0	A
TEC Voltage	V_C	$\Delta T = 40$°C	–	–	2.0	V

D.1.3 RF characteristics and distortion

Parameter	Symbol	Test Conditions	Min	Typ	Max	Unit
Frequency Range	F	–	45	–	550	MHz
Frequency Response	$\|S_{21}\|$	$I = 82$ mA $f = 45$-860 MHz $T = 25$°C	–	±0.5	–	dB
Carrier to Noise Ratio	CNR	Note 1	51	–	–	dB
Composite Second Order	CSO	Note 1	–	–	−64	dBc
Composite Triple Beat	CTB	Note 1	–	–	−70	dBc

Note 1: Test condition: $P_o = P_r$, OMI 2.8%, 77 unmodulated carriers (50 to 550 MHz), received power= −1dBm.

D.1.4 Test data

Parameter	Value	Unit
Operating Temperature	25	℃
Thermistor Resistance	10	KΩ
Optical Output Power	22	mW
Operating Current	74.6	mA
Monitor Current	300.2	µA
Threshold Current	12.6	mA
Slope Efficiency	0.35	W/A
Center Wavelength	1310.6	nm
SMSR	47.6	dB
RF Input	87.5	dBµV
OMI	3.2	%
CSO (lower band)	−64	dBc
CSO (upper band)	−65	dBc
CTB	−74	dBc
CNR	53	dB

Test condition CNR/CSO/CTB: NTSC-110 channel loading (50 to 750 MHz), −1 dBm received power.

D.2 Laser module B

Below are the datasheet specifications and the specific manufacturer test results of the 1310-nm laser module B used for the measurements in this project.

D.2.1 Absolute maximum ratings

Parameter	Symbol	Min	Max	Unit
Power Supply Voltage	V_{cc}	−0.5	7.0	V
Power Supply Voltage	V_{ee}	−7.0	0.5	V
Power Supply Current	I_{cc}	–	0.8	A
Power Supply Current	I_{ee}	–	1.2	A
Input Voltage	–	0	V_{cc}	V
RF Modulation per Channel (75Ω)	–	–	0	dBm
Storage Case Temperature Range	T_{stg}	−40	85*	°C

*2000 hours maximum

D.2.2 Recommended operating conditions

Parameter	Symbol	Min	Max	Unit
Power Supply Voltage	V_{cc}	4.5	5.5	V
Power Supply Voltage	V_{ee}	−5.5	−4.5	V
Operating Humidity	H_{opr}	5	95	%
Operating Temperature Range	T_A	−10	60	°C

D.2.3 Optical characteristics

Parameter	Symbol	Test Conditions	Min	Typ	Max	Unit
Optical Output Power	P_o	–	3.0	–	25.0	mW
Center Wavelength	λ_c	–	1290	1310	1330	nm
Optical Isolation	–	−10°C to +60°C	25	–	–	dB
Side-Mode Suppression Ratio	SMSR	Modulated	30	–	–	dB

D.2.4 Electrical characteristics

Parameter	Symbol	Test Conditions	Min	Typ	Max	Unit
Laser Forward Voltage	V_{lf}	At rated power	–	1.3	1.8	V
Laser Operating Current	I_{op}	–	–	50	100	mA
Threshold Current	I_{th}	*	–	10	30	mA
TEC Current	I_{TEC}	$\Delta T = 40$°C	–	–	1.0	A
TEC Voltage	V_{TEC}	$\Delta T = 40$°C	–	–	1.8	V
TEC Cooling Capacity	ΔT	–	40	–	–	°C

*The laser threshold current is the current at which the first derivative of the laser light vs. forward current is at one-half of its maximum.

D.2.5 Test data

Parameter	Value	Unit
Operating Temperature	25	°C
Optical Output Power	10.55	mW
Laser Bias Current	52.6	mA
Center Wavelength	1310 ± 10	nm
RF Input	98.0	dBµV
RF Flatness	±0.39	dB
OMI	2.9	%
CSO (lower band)	−64.4	dBc
CSO (upper band)	−65.9	dBc
CTB	−67	dBc
CNR	51	dB

Test condition CNR/CSO/CTB: PAL-D 84 channel loading (70 to 790 MHz), −1 dBm received power.

Appendix E

Additional measurements results

This appendix lists graphs for additional measurement results, that were not included in the body of the report for reasons of readability.

E.1 CNR Measurements

CNR fitting measurements for laser module *A*. Compare with Fig. 4.4 on page 32.

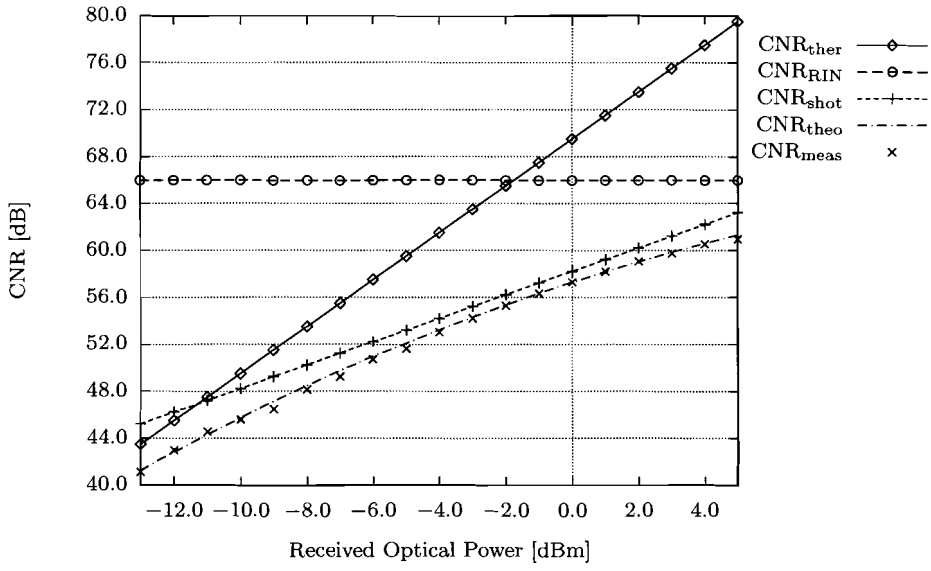

Figure E.1: Measured CNR versus received optical power for *Module A*, fitted with theoretical values for CNR and its individual components.
Fitted values: $OMI \approx 5.0\%$, $\sqrt{\langle i_{th}^2 \rangle} = 4.5pA/\sqrt{Hz}$, $RIN = -162dB/Hz$; $P_{rf} = 93.5dB\mu V/ch$
Measured at: $f = 119.25MHz$, $P_{opt,laser} = 13.1dBm$

E.2 CSO/CTB Measurements

Additional measurements done with both the two-tone measurement setup and the multi-tone generator. The two figures below allow a comparison to be made between intermodulation distortion as measured using a two-tone setup and the composite distortion measurements made with a multi-tone generator. As we have concluded, it is not possible to use standard 'multiply-by-number-of-distortion-products' theory to predict CSO and CTB from two-tone measurements.

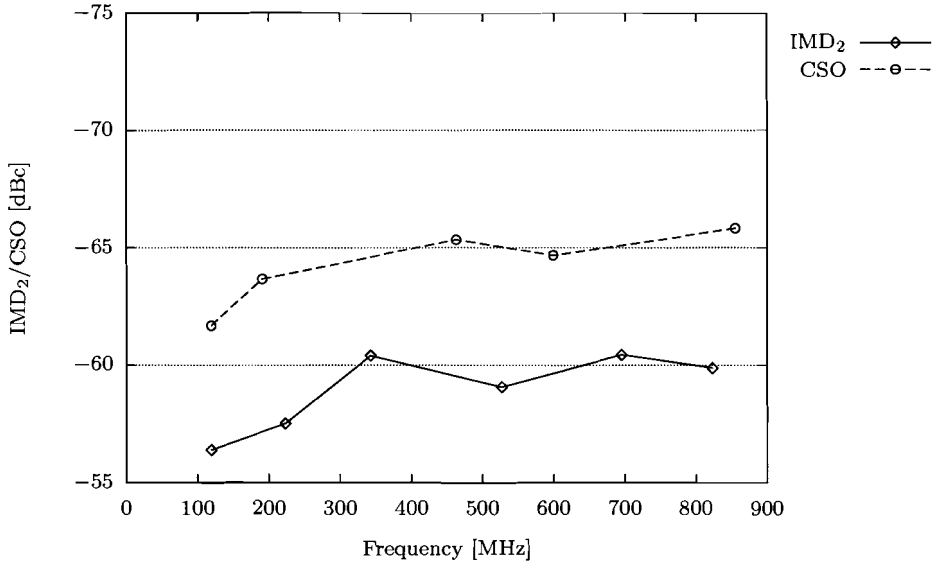

Figure E.2: Comparing CSO and IMD_2 performance for *Module B.* $P_{opt} = -6dBm$

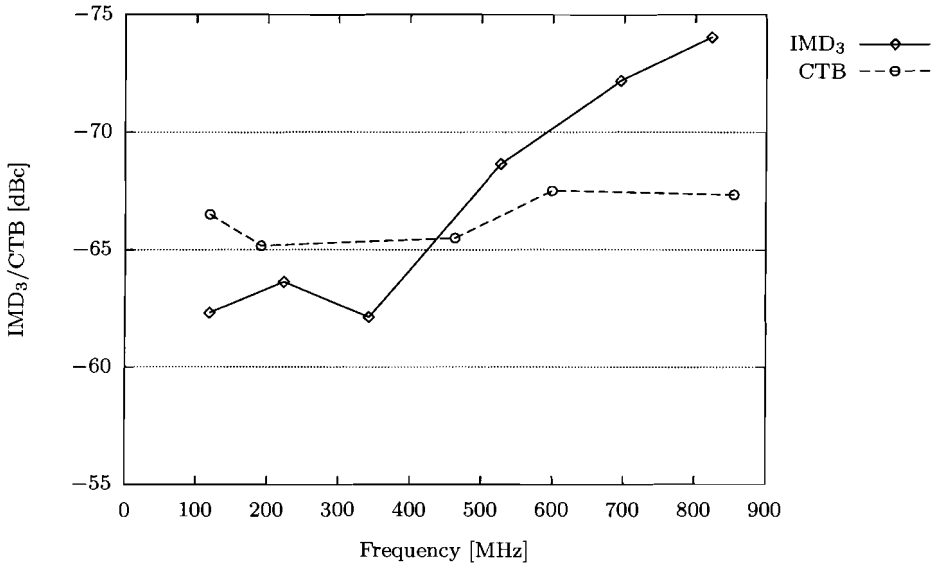

Figure E.3: Comparing CTB and IMD_3 performance for *Module B.* $P_{opt} = -6dBm$

Distortions over the received optical power input range. As we can see, distortions are relatively constant over the operating range. The low performance at $P_{opt} = -10\,\text{dBm}$ can be attributed to the spectrum analyzer, which is not sensitive enough to measure at low powers. For higher optical powers, receiver saturation will cause more distortions and thus higher CSO/CTB.

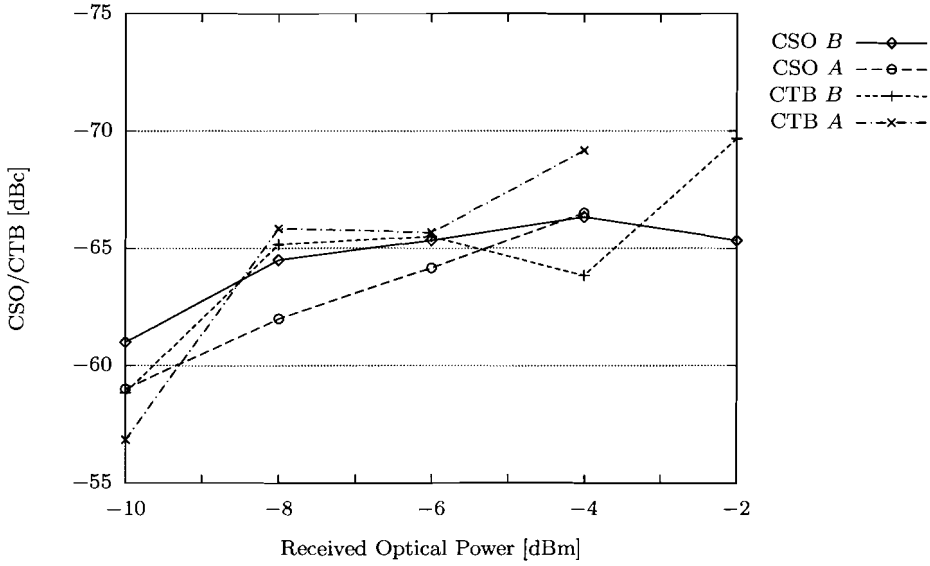

Figure E.4: CSO and CTB versus received optical power for both A and B modules. $f = 463.25 MHz$

Appendix F

Single Fiber FTTH

This appendix is released under embargo of one year after publication date. It contains more detailed information that is left out of Chapter 6.

F.1 CATV detector with data overlay

For the modular CPE, a special CATV photodetector is examined. This detector is manufactured by NSG Europe N.V. and has two fibers: one incoming fiber and one outgoing fiber. On the incoming fiber, both 1310/1490 nm data and 1550 nm CATV are present. Before the actual detector, a gradient-index (GRIN) lens and an WDM edge filter are placed to reflect both 1310 and 1490 nm into the outgoing fiber and pass the 1550 nm CATV signal to the photodetector. A schematic of this device is shown in Fig. F.1.

The most important property of this detector is the isolation between the data and CATV signals. For this device an isolation of at least 40 dB from data to CATV is guaranteed by the manufacturer.

For testing purposes and for building a system demonstrator, we have installed this special photodiode in a Genexis NTUO receiver. In Fig. F.2, the response of both the normal NTUO receiver and the modified one are displayed. This test is carried out using a 1554 nm externally modulated CATV laser and a HP8753E network analyzer. As we can see, the difference in response is about 1 dB for low frequencies up to almost 3 dB for high frequencies. Because the detector is an initial sample, we contacted the manufacturer to see how this lower responsivity (which translates in worse CNR performance) can be improved. It is clear that a 3-dB system penalty is not acceptable: for the same performance, we would need twice as much amplification. The manufacturer however assured us that the performance was due to the actual photodetector that is used in the package and not due to GRIN lens or WDM edge filter. Insertion loss for the lens and filter should be, according to the manufacturer specifications, lower than 0.25 dB. The performance as plotted in Fig. F.2 is therefore expected to improve substantially, when a better analog detector is used.

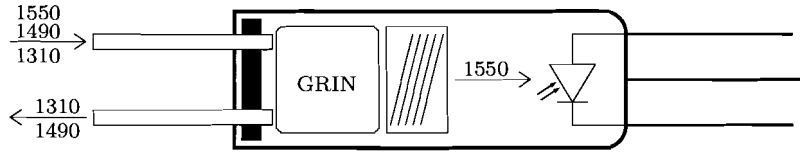

Figure F.1: Schematic of the NSG detector with GRIN lens and WDM edge filter.

F.2 Data BiDi with CATV overlay

In an effort to overcome the problem of the CO side of the single fiber system described in the previous section, we will now look at another device, which promises to keep the modular approach and fix the multiplexing problem.

This device, manufactured by Lightron Fiber-Optic Devices Inc., is a 1310/1490 nm 1.25 Gbit/s data transceiver with analog optical CATV overlay. The only disadvantage this device has, is that it is not combined with driver electronics for data communication and fit inside a SFP. It can therefore not immediately (or with minor changes) be deployed on existing PCB's. This and the fact that the samples for this device arrived in the last month of this project, was the reason why there was insufficient time to perform measurements with these modules and build them into a system demonstrator.

The Lightron datasheet promises an optical isolation of maximum −30 dB for CATV to data and vice versa, and a crosstalk (from a 1310 nm laser) of maximum −47 dB. As we have seen before, this easily matches the theoretical requirements and will match (or even surpass) the NSG isolation performance. Another advantage of this solution is that it is specified to have an insertion loss of 1.2 dB which, combined with a good CATV photodetector, yields a better system performance and therefore higher link budget.

Using this device, a gigabit optical ethernet switch with optical analog CATV overlay for use in the CO of a single fiber architecture becomes a viable possibility (see Fig. F.3).

It should be noted that this proposed switch also solves the missing CO solution when the NSG detector for the CPE is used. This would mix the two single-fiber solutions and create both an easy to use modular CPE solution and a cost-effective and viable CO solution. A central office demonstrator based on this schematic will be built in the near future.

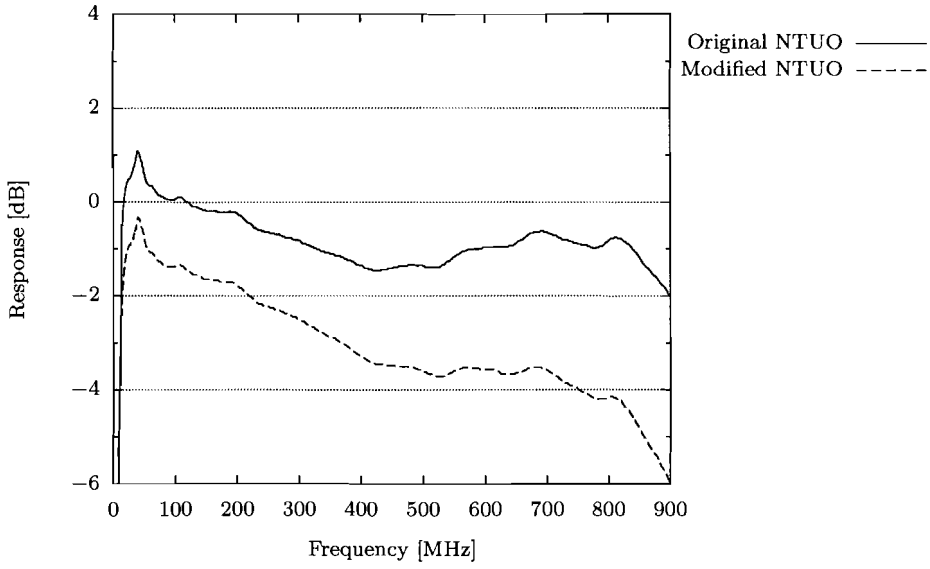

Figure F.2: Frequency response plot of the NTUO receiver before and after modification with the selective detector. Measured using a HP8753E network analyzer.

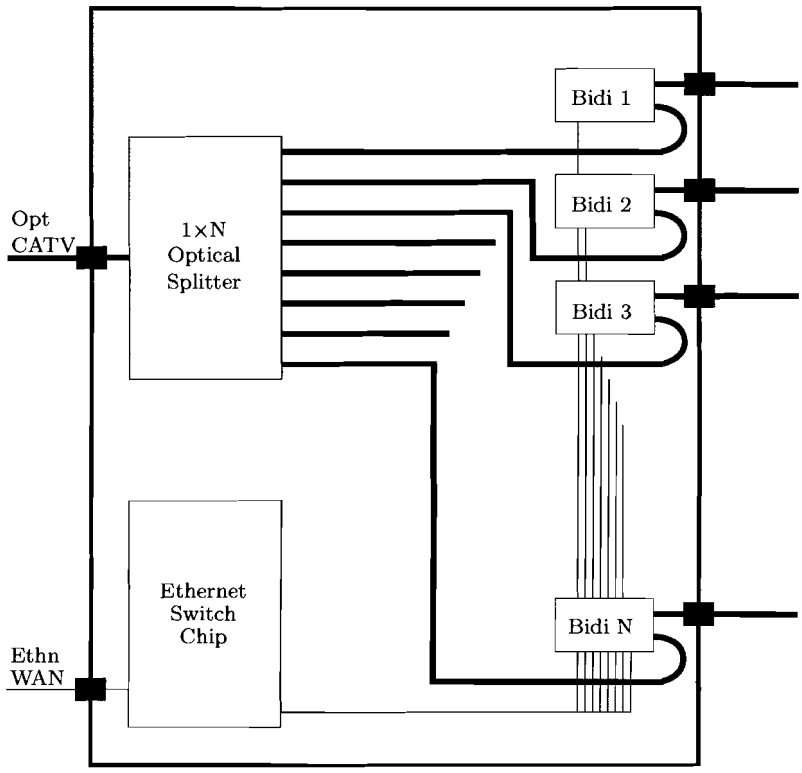

Figure F.3: Schematic of a gigabit optical ethernet switch with optical analog CATV overlay.

References

[1] "NTUO-801m modular optical CATV receiver datasheet," Genexis BV, Eindhoven, The Netherlands.

[2] H. T. Lin and Y. H. Kao, "Nonlinear distortions and compensations of DFB laser diode in AM-VSB lightwave CATV applications," *J. Lightwave Technol.*, vol. 14, pp. 2567–2574, Nov. 1996.

[3] J. Lipson *et al.*, "High-fidelity lightwave transmission of multiple AM-VSB NTSC signals," *IEEE Trans. Microwave Theory Tech.*, vol. 38, pp. 483–493, May 1990.

[4] C. Y. Kuo and E. E. Bergmann, "Second-order distortion and electronic compensation in analog links containing fiber amplifiers," *J. Lightwave Technol.*, vol. 10, pp. 1751–1759, Nov. 1992.

[5] A. A. M. Saleh, "Fundamental limit on number of channels in subcarrier-multiplexed lightwave CATV system," *Electron. Lett.*, vol. 25, no. 12, pp. 776–777, June 1989.

[6] K. Ho and J. M. Kahn, "On models of clipping distortion for lightwave CATV systems," *IEEE Photon. Technol. Lett.*, vol. 8, pp. 125–126, Jan. 1996.

[7] N. J. Frigo, M. R. Phillips, and G. E. Bodeep, "Clipping distortion in lightwave CATV systems: models, simulations, and measurements," *J. Lightwave Technol.*, vol. 11, pp. 138–146, Jan. 1993.

[8] N. A. Olsson, "Lightwave systems with optical amplifiers," *J. Lightwave Technol.*, vol. 7, pp. 1071–1082, July 1989.

[9] W. I. Way, "Subcarrier multiplexed lightwave system design considerations for subscriber loop applications," *J. Lightwave Technol.*, vol. 7, pp. 1806–1818, Nov. 1989.

[10] P. Wan and J. Conradi, "Impact of double Rayleigh backscatter noise on digital and analog fiber systems," *J. Lightwave Technol.*, vol. 14, pp. 288–297, Mar. 1996.

[11] *Cable networks for television signals, sound signals and interactive services - Part 7: system performance*, EN Std. 50 083-7, 2000.

[12] A. M. J. Koonen, *Handboek Elektrotechniek: Transmissie via optische geleiders.* Alphen a/d Rijn, The Netherlands: Samsom Bedrijfsinformatie, 2003, pp. 140–151.

[13] *Cable networks for television signals, sound signals and interactive services - Part 3: active wideband equipment for coaxial cable networks*, EN Std. 50 083-3, 2002.

[14] W. I. Way, *Broadband hybrid fiber/coax access system technologies.* San Diego, CA: Academic Press, 1999, pp. 33–37.

[15] M. R. Phillips, T. E. Darcie, D. Marcuse, G. E. Bodeep, and N. J. Frigo, "Nonlinear distortion generated by dispersive transmission of chirped intensity-modulated signals," *IEEE Photon. Technol. Lett.*, vol. 3, no. 5, pp. 481–483, May 1991.

[16] E. E. Bergmann, C. Y. Kuo, and S. Y. Huang, "Dispersion-induced composite second order distortion at 1.5 μm," *IEEE Photon. Technol. Lett.*, vol. 3, no. 1, pp. 59–61, Jan. 1991.

[17] H. Yonetani, I. Ushijima, T. Takada, and K. Shima, "Transmission characteristics of DFB laser modules for analog applications," *J. Lightwave Technol.*, vol. 11, pp. 147–153, Jan. 1993.

[18] Y. Aoki, K. Tajima, and I. Mito, "Input power limits of single-mode optical fibers due to Stimulated Brillouin Scattering in optical communication systems," *IEEE Photon. Technol. Lett.*, vol. 6, no. 5, pp. 710–719, May 1988.

[19] F. W. Willems, W. Muys, and J. S. Leong, "Simultaneous suppression of Stimulated Brillouin Scattering and interferometric noise in externally modulated lightwave AM-SCM systems," *IEEE Photon. Technol. Lett.*, vol. 6, no. 12, pp. 1476–1478, Dec. 1988.

[20] *Cable networks for television signals, sound signals and interactive services - Part 6: optical equipment*, EN Std. 50 083-6, 1998.

[21] *Semiconductor optoelectronic devices for fibre optic system applications - Part 2: measuring methods*, IEC Std. 62 007-2, Rev. 1.1, 1999.

[22] C. M. Miller, "Intensity modulation and noise characterization of high-speed semiconductor lasers," *IEEE J. Lightwave Telecomm. Syst.*, vol. 2, pp. 44–53, May 1991.

[23] W. Muys, J. C. van der Plaats, F. W. Willems, *et al.*, "A 50-channel externally modulated AM-VSB video distribution system with three cascaded EDFA's providing 50-dB power budget over 30 km of standard single-mode fiber," *IEEE Photon. Technol. Lett.*, vol. 7, no. 6, pp. 691–693, June 1995.

[24] R. Schoop, F. Fredricx, A. M. J. Koonen, and C. Hardalov, "WDM isolation requirements for CATV in BPON," in *Proc. ECOC'02, Paper 9.2.6*, Copenhagen, Denmark, Sept. 2002, pp. 1–2.

Acknowledgement

Following an email of Prof. Djan Khoe, head of the ECO group, a meeting was held with Prof. Ton Koonen of ECO and Gerlas van den Hoven of Genexis. In this meeting my graduation project was born and Gerlas gave me the opportunity to come work at Genexis for a period of 9 months to do research and write my thesis. I am grateful for the opportunity to work in a startup company in the optical telecommunications field and see the development of FTTH from close range.

I would especially like to thank my supervisor at Genexis, Hans Crijns, for his good advice and help during this project. However busy he was, I could always ask him for advice. Although I worked very independently for most of the time, the few times I was stuck, he always took the time to help me get going again. The regular progress discussions with him guided my direction and kept me focussed on the targets.

During this project, I have worked together with people at BTI Bremi several times. I would like to thank Peter Fober for his background information on CATV theory and measurements. Most importantly, I would like to thank Pim van der Heijden for enabling and helping me to do several measurements at BTI Bremi, including CSO/CTB measurements using their multi-tone generator. Also, I want to thank him for his help and input with the realization of the single fiber demonstrator.

At the Eindhoven University of Technology, Peter van Bennekom generously lent me some RF components for the two-tone measurements and gave me advice on the purchase of other RF components. He also helped me to carry out the laser RIN measurements, which were conducted at the University.

My graduation professor and supervisor from the university was Ton Koonen. His feedback on my work was very useful, especially when dealing with the theoretical background and in the last phase of my project, when I was writing this report.

Last but not least I want to thank my co-workers at Genexis for the great time I have had there. Carla, Peter, Gerlas, Hans, Maarten and Ward: I hope you will do well, both in business and in your personal lives. And who knows, our roads might cross again somewhere in the future...